Sakahira, H., Enari, M., and Nagata, S. (1998). Cleavage of CAD inhibitor in CAD activation and DNA degradation during apoptosis. Nature *391*, 96–99.

Sakahira, H., Iwamatsu, A., and Nagata, S. (2000). Specific chaperone-like activity of inhibitor of caspase-activated DNase for caspase-activated DNase. J. Biol. Chem. *275*, 8091–8096.

Sakahira, H., Takemura, Y., and Nagata, S. (2001). Enzymatic active site of caspase-activated DNase (CAD) and its inhibition by inhibitor of CAD. Arch. Biochem. Biophys. *388*, 91–99.

Samejima, K., Tone, S., and Earnshaw, W.C. (2001). CAD/DFF40 nuclease is dispensable for high molecular weight DNA cleavage and stage I chromatin condensation in apoptosis. J. Biol. Chem. *276*, 45427–45432.

Schlegel, R.A., and Williamson, P. (2007). P.S. to PS (phosphatidylserine)—pertinent proteins in apoptotic cell clearance. Sci. STKE *2007*, pe57.

Scott, R.S., McMahon, E.J., Pop, S.M., Reap, E.A., Caricchio, R., Cohen, P.L., Earp, H.S., and Matsushima, G.K. (2001). Phagocytosis and clearance of apoptotic cells is mediated by MER. Nature *411*, 207–211.

Sebbagh, M., Renvoizé, C., Hamelin, J., Riché, N., Bertoglio, J., and Bréard, J. (2001). Caspase-3-mediated cleavage of ROCK I induces MLC phosphorylation and apoptotic membrane blebbing. Nat. Cell Biol. *3*, 346–352.

Shakhov, A.N., Rybtsov, S., Tumanov, A.V., Shulenin, S., Dean, M., Kuprash, D.V., and Nedospasov, S.A. (2004). SMUCKLER/TIM4 is a distinct member of TIM family expressed by stromal cells of secondary lymphoid tissues and associated with lymphotoxin signaling. Eur. J. Immunol. *34*, 494–503.

Strasser, A., Jost, P.J., and Nagata, S. (2009). The many roles of FAS receptor signaling in the immune system. Immunity *30*, 180–192.

Su, H.P., Nakada-Tsukui, K., Tosello-Trampont, A.C., Li, Y., Bu, G., Henson, P.M., and Ravichandran, K.S. (2002). Interaction of CED-6/GULP, an adapter protein involved in engulfment of apoptotic cells with CED-1 and CD91/low density lipoprotein receptor-related protein (LRP). J. Biol. Chem. *277*, 11772–11779.

Susin, S.A., Daugas, E., Ravagnan, L., Samejima, K., Zamzami, N., Loeffler, M., Costantini, P., Ferri, K.F., Irinopoulou, T., Prévost, M.C., et al. (2000). Two distinct pathways leading to nuclear apoptosis. J. Exp. Med. *192*, 571–580.

Suzuki, M., Sugimoto, Y., Ohsaki, Y., Ueno, M., Kato, S., Kitamura, Y., Hosokawa, H., Davies, J.P., Ioannou, Y.A., Vanier, M.T., et al. (2007). Endosomal accumulation of Toll-like receptor 4 causes constitutive secretion of cytokines and activation of signal transducers and activators of transcription in Niemann-Pick disease type C (NPC) fibroblasts: a potential basis for glial cell activation in the NPC brain. J. Neurosci. *27*, 1879–1891.

Taberner, M., Scott, K.F., Weininger, L., Mackay, C.R., and Rolph, M.S. (2005). Overlapping gene expression profiles in rheumatoid fibroblast-like synoviocytes induced by the proinflammatory cytokines interleukin-1 beta and tumor necrosis factor. Inflamm. Res. *54*, 10–16.

Tada, K., Tanaka, M., Hanayama, R., Miwa, K., Shinohara, A., Iwamatsu, A., and Nagata, S. (2003). Tethering of apoptotic cells to phagocytes through binding of CD47 to Src homology 2 domain-bearing protein tyrosine phosphatase substrate-1. J. Immunol. *171*, 5718–5726.

Tanaka, Y., and Schroit, A.J. (1983). Insertion of fluorescent phosphatidylserine into the plasma membrane of red blood cells. Recognition by autologous macrophages. J. Biol. Chem. *258*, 11335–11343.

Timmer, J.C., and Salvesen, G.S. (2007). Caspase substrates. Cell Death Differ. *14*, 66–72.

Trouw, L.A., Blom, A.M., and Gasque, P. (2008). Role of complement and complement regulators in the removal of apoptotic cells. Mol. Immunol. *45*, 1199–1207.

Truman, L.A., Ogden, C.A., Howie, S.E., and Gregory, C.D. (2004). Macrophage chemotaxis to apoptotic Burkitt's lymphoma cells in vitro: role of CD14 and CD36. Immunobiology *209*, 21–30.

Truman, L.A., Ford, C.A., Pasikowska, M., Pound, J.D., Wilkinson, S.J., Dumitriu, I.E., Melville, L., Melrose, L.A., Ogden, C.A., Nibbs, R., et al. (2008). CX3CL1/fractalkine is released from apoptotic lymphocytes to stimulate macrophage chemotaxis. Blood *112*, 5026–5036.

Tsujimoto, Y., and Shimizu, S. (2005). Another way to die: autophagic programmed cell death. Cell Death Differ. *12 (Suppl 2)*, 1528–1534.

Uematsu, S., and Akira, S. (2007). Toll-like receptors and Type I interferons. J. Biol. Chem. *282*, 15319–15323.

Umetsu, S.E., Lee, W.L., McIntire, J.J., Downey, L., Sanjanwala, B., Akbari, O., Berry, G.J., Nagumo, H., Freeman, G.J., Umetsu, D.T., and DeKruyff, R.H. (2005). TIM-1 induces T cell activation and inhibits the development of peripheral tolerance. Nat. Immunol. *6*, 447–454.

van den Eijnde, S.M., Boshart, L., Baehrecke, E.H., De Zeeuw, C.I., Reutelingsperger, C.P., and Vermeij-Keers, C. (1998). Cell surface exposure of phosphatidylserine during apoptosis is phylogenetically conserved. Apoptosis *3*, 9–16.

Venegas, V., and Zhou, Z. (2007). Two alternative mechanisms that regulate the presentation of apoptotic cell engulfment signal in Caenorhabditis elegans. Mol. Biol. Cell *18*, 3180–3192.

Wang, X., Wu, Y.C., Fadok, V.A., Lee, M.C., Gengyo-Ando, K., Cheng, L.C., Ledwich, D., Hsu, P.K., Chen, J.Y., Chou, B.K., et al. (2003). Cell corpse engulfment mediated by C. elegans phosphatidylserine receptor through CED-5 and CED-12. Science *302*, 1563–1566.

Ward, P.P., Mendoza-Meneses, M., Cunningham, G.A., and Conneely, O.M. (2003). Iron status in mice carrying a targeted disruption of lactoferrin. Mol. Cell. Biol. *23*, 178–185.

Woo, E.-J., Kim, Y.-G., Kim, M.-S., Han, W.-D., Shin, S., Robinson, H., Park, S.-Y., and Oh, B.-H. (2004). Structural mechanism for inactivation and activation of CAD/DFF40 in the apoptotic pathway. Mol. Cell *14*, 531–539.

Wyllie, A.H. (1980). Glucocorticoid-induced thymocyte apoptosis is associated with endogenous endonuclease activation. Nature *284*, 555–556.

Xiong, W., Chen, Y., Wang, H., Wang, H., Wu, H., Lu, Q., and Han, D. (2008). Gas6 and the Tyro 3 receptor tyrosine kinase subfamily regulate the phagocytic function of Sertoli cells. Reproduction *135*, 77–87.

Yamaguchi, H., Takagi, J., Miyamae, T., Yokota, S., Fujimoto, T., Nakamura, S., Ohshima, S., Naka, T., and Nagata, S. (2008). Milk fat globule EGF factor 8 in the serum of human patients of systemic lupus erythematosus. J. Leukoc. Biol. *83*, 1300–1307.

Yokota, S., Imagawa, T., Mori, M., Miyamae, T., Aihara, Y., Takei, S., Iwata, N., Umebayashi, H., Murata, T., Miyoshi, M., et al. (2008). Efficacy and safety of tocilizumab in patients with systemic-onset juvenile idiopathic arthritis: a randomised, double-blind, placebo-controlled, withdrawal phase III trial. Lancet *371*, 998–1006.

Yoshida, H., Kawane, K., Koike, M., Mori, Y., Uchiyama, Y., and Nagata, S. (2005a). Phosphatidylserine-dependent engulfment by macrophages of nuclei from erythroid precursor cells. Nature *437*, 754–758.

Yoshida, H., Okabe, Y., Kawane, K., Fukuyama, H., and Nagata, S. (2005b). Lethal anemia caused by interferon-beta produced in mouse embryos carrying undigested DNA. Nat. Immunol. *6*, 49–56.

Zhang, H.G., Hyde, K., Page, G.P., Brand, J.P., Zhou, J., Yu, S., Allison, D.B., Hsu, H.C., and Mountz, J.D. (2004). Novel tumor necrosis factor alpha-regulated genes in rheumatoid arthritis. Arthritis Rheum. *50*, 420–431.

Züllig, S., Neukomm, L.J., Jovanovic, M., Charette, S.J., Lyssenko, N.N., Halleck, M.S., Reutelingsperger, C.P., Schlegel, R.A., and Hengartner, M.O. (2007). Aminophospholipid translocase TAT-1 promotes phosphatidylserine exposure during C. elegans apoptosis. Curr. Biol. *17*, 994–999.

 DOI 10.1002/eji.200940096 Eur. J. Immunol. 2010. 40: 1778–1785

Aberrant splicing of the milk fat globule-EGF factor 8 (MFG-E8) gene in human systemic lupus erythematosus

Hiroshi Yamaguchi[1,2], Takashi Fujimoto[3], Shinobu Nakamura[3], Koichiro Ohmura[4], Tsuneyo Mimori[4], Fumihiko Matsuda[5] and Shigekazu Nagata[1,2,6]

[1] Department of Medical Chemistry, Graduate School of Medicine, Kyoto University, Sakyo, Kyoto, Japan
[2] Department of Integrated Biology, Graduate School of Frontier Bioscience, Osaka University, Osaka, Japan
[3] Department of General Medicine, Nara Medical University, Kashihara, Nara, Japan
[4] Department of Rheumatology and Clinical Immunology, Graduate School of Medicine, Kyoto University, Sakyo, Kyoto, Japan
[5] Center for Genomic Medicine/Inserm U.852, Graduate School of Medicine, Kyoto University, Sakyo, Kyoto, Japan
[6] Core Research for Evolutional Science and Technology, Japan Science and Technology Corporation, Sakyo, Kyoto, Japan

Milk fat globule-EGF factor 8 (MFG-E8) promotes the phagocytosis of apoptotic cells by serving as a bridging molecule between apoptotic cells and phagocytes. Many apoptotic cells are left unengulfed in the germinal centers of the spleen of MFG-E8$^{-/-}$ mice, which develop a human systemic lupus erythematosus (SLE)-like autoimmune disease. Here, we analyzed the MFG-E8 gene in human SLE patients, and found in two out of 322 female patients a heterozygous intronic mutation, which caused a cryptic exon from intron 6 to be included in the transcript. The cryptic exon contained a premature termination codon, generating a C-terminally truncated MFG-E8 protein. The mutant MFG-E8 was aberrantly glycosylated and sialylated, but bound to phosphatidylserine and enhanced the phagocytosis of apoptotic cells. When intravenously injected into mice, the mutant MFG-E8 was sustained longer in the blood circulation than wild-type MFG-E8. Repeated administrations of the mutant MFG-E8 protein induced the production of autoantibodies, such as anti-cardiolipin and anti-nuclear antibodies, at a lower dose than that required for the wild-type protein. These results suggested that the intronic mutation in the human MFG-E8 gene can lead to the development of SLE.

Key words: Aberrant splicing · Apoptosis · Autoimmiune disease · Protein stability

Introduction

Unnecessary or harmful cells are eliminated by apoptosis, a form of programmed cell death in which cysteine proteases of the caspase family are activated to cleave cellular substrates [1, 2]. The apoptotic cells are rapidly engulfed and digested by phagocytes such as macrophages and immature dendritic cells. The swift engulfment of cell corpses by phagocytes prevents the release of noxious or immunogenic debris from dying cells into the circulation. In the process of apoptosis, the dying cells expose phosphatidylserine on their external membrane in a caspase-dependent manner. This externalization of phosphatidylserine is

Correspondence: Professor Shigekazu Nagata
e-mail: snagata@mfour.med.kyoto-u.ac.jp

one of the hallmarks of apoptosis and acts as an "eat me" signal for phagocytes [3]. Recently, several molecules that recognize phosphatidylserine have been identified [4–7].

Systemic lupus erythematosus (SLE) is a chronic autoimmune disease caused by multiple genetic and environmental factors [8]. Patients with SLE develop a broad spectrum of clinical manifestations affecting the skin, kidney, lungs, blood vessels, and/or nervous system. SLE is also characterized by the presence in sera of autoantibodies against nuclear components (anti-RNP and anti-DNA antibodies). Unengulfed apoptotic cells can be found in the germinal centers of the lymph nodes of some SLE patients, and macrophages from these patients show a reduced ability to engulf apoptotic cells [9]. Furthermore, circulating DNA or nucleosomes can also be found in the sera of SLE patients [10, 11]. These results suggest that a deficiency in the clearance of apoptotic cells is one of the causes of SLE.

Milk fat globule-EGF factor 8 (MFG-E8) is a glycoprotein. At the *N*-terminus, it has a EGF-like repeat(s), and at the *C*-terminus, there are two discoidin domains that bind phosphatidylserine. It was originally identified as a component of milk fat globules that bud from the mammary epithelia during lactation. But it is now known to play important roles in various systems such as involution of mammary glands, adhesion between sperm and egg, repair of intestinal mucosa, and angiogenesis [12]. MFG-E8 is secreted by activated macrophages and immature dendritic cells [13], and it promotes the engulfment of apoptotic cells by working as a bridging molecule between apoptotic cells and phagocytes [7]. In MFG-E8-knockout mice, many apoptotic cells are left unengulfed in the germinal centers of the spleen [14]. The MFG-E8$^{-/-}$ mice produce autoantibodies including anti-cardiolipin and anti-dsDNA antibodies and suffer from an SLE-type autoimmune disease. Human MFG-E8 is maintained at the optimal concentration to support the engulfment of apoptotic cells; in excess, MFG-E8 inhibits phagocytosis and causes autoimmune diseases [15, 16].

In this report, we analyzed the human MFG-E8 gene of SLE patients, and found in two female patients an intronic mutation that caused aberrant splicing of intron 6, resulting in the inclusion of a cryptic exon in the transcript. This cryptic exon contained a premature termination codon, which generated an MFG-E8 mutant truncated at the C2-homologous domain. The truncated MFG-E8 (designated as C2del) was abnormally glycosylated with terminal sialic acids; yet, it bound to phosphatidylserine and enhanced the phagocytosis of apoptotic cells. When injected into mice, C2del showed greater stability than wild-type MFG-E8 and induced the production of autoantibodies, suggesting that this mutation of the MFG-E8 gene can lead to the development of SLE in humans.

Results

Analysis of MFG-E8 mRNA in human SLE patients

The human MFG-E8 gene is located on human chromosome 15q25 and is composed of eight exons (National Center for Biotechnology Information GenBank Accession Number WC_000015). To sequence the coding regions of human MFG-E8 gene in a cohort of Japanese female SLE patients ($n = 110$), cDNA was prepared from RNA isolated from the patients' peripheral blood mononuclear cells. Two sets of PCR primers, which amplified the cDNA corresponding to exons 1–5, and exons 4–8 of the human MFG-E8 gene, were prepared (Fig. 1A). No abnormality was found in the cDNA corresponding to the first set of exons (exons 1–5) in any of the 110 patients, but the RT-PCR of exons 4–8 from one patient yielded a longer-than-normal amplicon in addition to the wild-type one (Fig. 1B). A sequence analysis and BLAST search indicated that the long amplicon contained a cryptic exon of 102 bp from intron 6 of the MFG-E8 gene (Fig. 1C). This insertion caused a premature termination of the human MFG-E8 coding sequence.

Aberrant splice-in of a cryptic exon caused by an A-to-G mutation in intron 6

Exons are defined by exonic and intronic *cis*-regulatory elements in addition to the core splice-site motifs [17, 18]. A sequence analysis of the human MFG-E8 chromosomal gene of the patient revealed a heterozygous A-to-G point mutation located 43 bp downstream of the cryptic exon, or 937 bp from exon 5 (IVS 6-937) (Fig. 1C and D). To examine the effect of this point mutation on the pre-mRNA splicing of the human MFG-E8 gene, an MFG-E8 minigene carrying intron 6 was constructed (Fig. 2A). That is, a part of exon 6–7 of the human MFG-E8 cDNA, in pEF-BOS vector [19], was replaced by a DNA fragment of the human MFG-E8 chromosomal gene carrying exon 6, intron 6, and exon 7 from the patient (G-allele at IVS 6-937) or a control (A-allele at IVS 6-937) individual (Fig. 2A). The splicing pattern of the MFG-E8 minigene was then assayed by expression in human HEp-2 cells. Semi-quantitative RT-PCR analysis of the RNA showed that the RNA carrying the cryptic exon was reproducibly about ten times more abundant in the cells transfected with the G-allele minigene than the cells transfected with the A-allele minigene (Fig. 2B). These results indicated that the A-to-G mutation in intron 6 (IVS 6-937 A>G) caused the aberrant inclusion of the cryptic exon in the human MFG-E8 transcript.

A screening of the MFG-E8 chromosomal gene by DNA sequencing revealed the same intronic mutation (IVS 6-937 A>G) in additional one patient out of 212 Japanese female SLE patients, while none of 228 healthy female volunteers carried the mutation.

C2del binds to phosphatidylserine and enhances the phagocytosis of apoptotic cells

Human MFG-E8 consists of a signal sequence, an EGF-like domain carrying an RGD motif, and two Factor VIII C1/C2-homologous domains (Fig. 3A). The MFG-E8 transcript that included the cryptic exon encoded an MFG-E8 protein that was truncated at the C2 domain (designated as C2del) (Fig. 3A). Studies on mouse and bovine MFG-E8 show that the C1/C2-

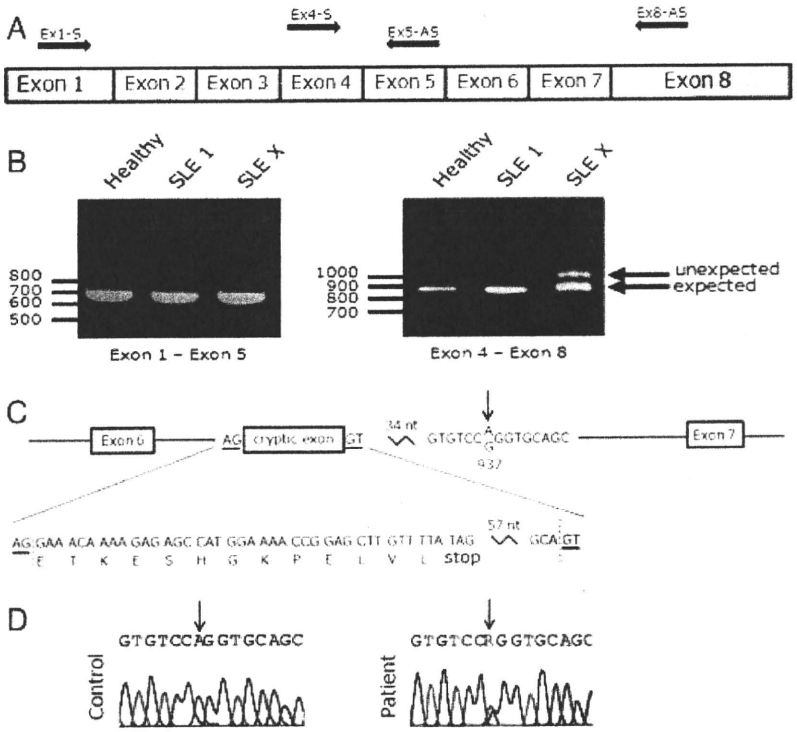

Figure 1. Sequence analysis of the human MFG-E8 gene in SLE patients. (A) Schematic presentation of the human MFG-E8 cDNA and the primers used for PCR. The 5′ and 3′ non-coding regions are indicated as blue boxes. (B) Agarose gel electrophoresis of the RT-PCR product from a healthy person and two SLE patients (SLE 1 and SLE X). PCR were performed with Ex1-S and Ex5-AS (left) or with Ex4-S and Ex8-AS (right). One hundred and ten SLE patients were examined. (C) A cryptic exon in intron 6 of the human MFG-E8 gene. The splice acceptor and donor sites (AG-GT) flanking the cryptic exon are underlined. A partial sequence of the cryptic exon is shown with the deduced amino acid sequence. IVS 6-937 is an A-to-G mutation located 43 bp downstream of the cryptic exon, and indicated by an arrow. (D) The sequence profile of IVS 6-937 and its flanking regions in a control subject (left) and in the patient (right). The position of IVS 6-937 is indicated by an arrow. The SNP in human MFG-E8 gene was submitted to NCBI dbSNP with the submitter SNP (ss) number 184955574.

homologous domains are required for binding to phosphatidylserine [7, 20]. To characterize C2del, we prepared human rMFG-E8 using HeLa cell transformants that produced the transgene in a tetracycline-dependent manner. On SDS-PAGE, the purified C2del ran as a smeared band of approximately 50 kDa, which was significantly bigger than the 46-kDa wild-type MFG-E8 (Fig. 3B). This was unexpected considering that C2del had a truncation of 96 amino acids and contained only one of three *N*-linked glycosylation sites present in the wild-type protein. The treatment of C2del with PNGase F reduced its molecular weight to 32.6 kDa (Fig. 3C), and a mutation of the remaining *N*-glycosylation site (Asn^{238}) also reduced its molecular weight (data not shown). Neuraminidase treatment significantly reduced C2del's molecular weight (Fig. 3D), indicating that it was sialylated. These results suggested that this C-terminal truncation of human MFG-E8 caused it to be aberrantly glycosylated.

We next examined the ability of C2del to recognize apoptotic cells. As shown in Fig. 3E, C2del dose-dependently bound to phosphatidylserine. The dissociation constants (Kd) determined by Biacore for the wild-type and C2del MFG-E8 were 1.1 and 8.0 nM, respectively. C2del supported phagocytosis with a bell-shaped dosage effect and the same dose dependency as the wild-type molecule (Fig. 3F). However, the ability of C2del to enhance the engulfment at the optimum concentration was consistently lower than that observed with the wild-type MFG-E8.

Aberrant *in vivo* stability of C2del and the induction of autoimmune disease

As described above, C2del was aberrantly glycosylated, and in particular, sialylated. The sialylation of proteins is known to prolong their half-life *in vivo* [21, 22]. To examine whether this was true for C2del, the wild-type MFG-E8 and C2del proteins were injected into C57BL/6 mice, and their levels in serum were monitored by ELISA. As shown in Fig. 4A, when 12 pmol of the wild-type or mutant MFG-E8 was injected into the tail vein, about 20 pM wild-type MFG-E8 was found in the serum after 60 min, whereas the concentration of C2del was more than 1 nM at the same time point. These results suggested that C2del was sustained longer than the wild-type protein in the blood.

We previously showed that excess MFG-E8 prevents the efficient engulfment of apoptotic cells and that some SLE patients carry a significantly increased level of MFG-E8 in their blood [15]. Accordingly, the injection of wild-type MFG-E8 into mice induced the development of autoimmune diseases [16]. Since C2del lasted

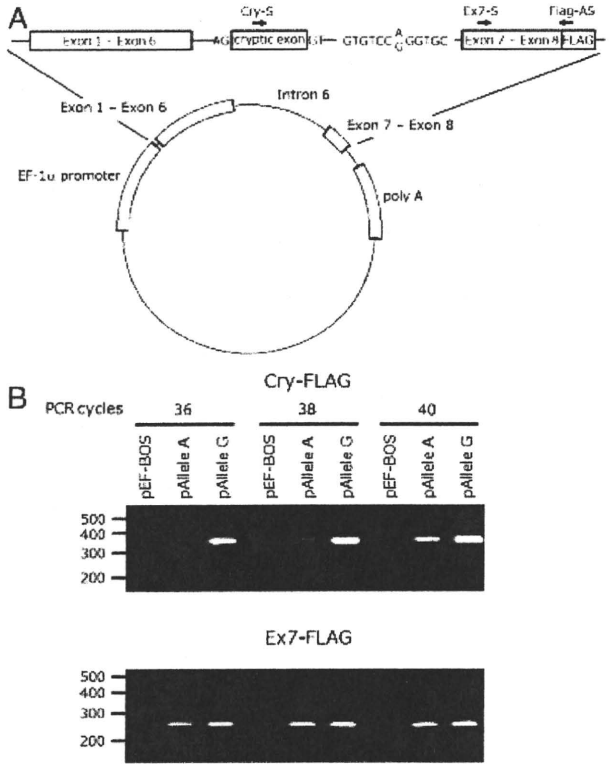

Figure 2. Inclusion of a cryptic exon in the MFG-E8 transcript caused by the IVS 6-937 A>G mutation. (A) Overall structure of the vector used to study the splicing of the MFG-E8 minigene. Human MFG-E8 minigenes, driven by the human EF-1α promoter, were constructed by inserting intron 6 of the A allele (control) and the G allele (patient) into the MFG-E8 cDNA. Positions of the primers (Cry-S, Ex7-S, and Flag-AS) for RT-PCR analysis are indicated by arrows. (B) RT-PCR for the RNA carrying the cryptic exon. The MFG-E8 minigene was transfected with HEp-2 cells, incubated overnight, and treated with 100 μg/mL cycloheximide for 2 h. RT-PCR with the total RNA was performed for the indicated cycles using the primers of Cry-S and Flag-AS (Cry-FLAG) to detect the cryptic exon (upper), or with the primers of Ex7-S and Flag-AS (Ex7-FLAG) to monitor the expression of exon 7 of the MFG-E8 minigene (lower). Transfection into HEp-2 cells and RT-PCR analysis were done independently three times, and representative data are shown.

longer *in vivo* than wild-type MFG-E8, we hypothesized that the administration of C2del might cause autoimmune disease in mice at a lower dose than the wild-type molecule. As shown in Fig. 4B, the repeated injection of C2del induced the production of anti-nuclear antibodies in mice at a dose, with which the wild-type MFG-E8 had little effect. In addition, two out of five mice injected with C2del developed a high level of anti-cardiolipin antibodies (Fig. 4C). These results suggested that C2del could be responsible for the development of SLE in the patient.

Discussion

Approximately 70% of human genes have alternatively spliced transcripts [23]. While alternative splicing generally facilitates the synthesis of a greater variety of proteins, mutations disrupting the splice sites or their regulatory elements can cause hereditary disease through the production of aberrant transcripts [24]. In this report, we described SLE patients whose MFG-E8 mRNA carry an insertion of 102 nt that resembles a cryptic exon. A splicing assay using a human MFG-E8 minigene carrying intron 6 revealed that the aberrant splicing of the MFG-E8 gene was caused by an A-to-G mutation in the intron. The inclusion of the cryptic exon in the transcript, as a result of this mutation, may be explained by the generation of a GGG motif, an intronic splicing enhancer [25, 26], which activates an exon choice by interacting with trans factors that regulate splicing [27, 28]

The cryptic exon incorporated in C2del had a premature termination codon located in the C2 domain of human MFG-E8. In general, mRNA that contain premature termination codons are eliminated by an mRNAs surveillance mechanism called nonsense-mediated mRNA decay (NMD) [29]. In fact, in a splicing assay with the MFG-E8 minigene, the transcripts containing the cryptic exon increased when the premature termination was blocked by treating the cells with cycloheximide or by removing the termination codon with site-directed mutagenesis (data not shown). On the other hand, a significant proportion of the MFG-E8 transcripts from the patient carried the cryptic exon. There are two possible explanations for this discrepancy: (i) the efficiency of NMD is different between HEp-2 and human peripheral blood mononuclear cells [30], and (ii) the mutant transcript may be more stable in the white blood cells of the patient. In addition, the NMD efficiency is known to differ among individuals. For example, the same mutation that leads to premature termination in the dystrophin gene can cause a mild (Becher muscular dystrophy) or more severe (Duchene muscular dystrophy) phenotype in different individuals [31].

Wild-type human MFG-E8 has an apparent M_r of 46 kDa, carries three *N*-glycosylation sites, and is glycosylated. C2del retained only one of the glycosylation sites, yet its molecular weight increased to 50 kDa, due to higher glycosylation. This aberrant glycosylation was observed in other cell lines, such as HEK293T cells (data not shown), confirming that it was an intrinsic property of C2del, and is not due to the host cell lines. The carbohydrate attached to C2del was sialylated, suggesting that the carbohydrate moiety was structurally different from that on the wild-type protein. Missense or truncation mutations in secreted or membrane proteins often cause to abnormal glycosylation and the accumulation of the proteins in the endoplasmic reticulum [32, 33]. We found that when C2del was expressed in HeLa cells, a significant portion of the product remained in the ER, where it was associated with calnexin and GRP78, ER chaperons (data not shown). It is possible that C2del was more heavily glycosylated and sialylated at ER to compensate for its insolubility.

SLE is an autoimmune disease characterized by the presence of autoantibodies, such as anti-nuclear and anti-DNA antibodies [8]. We previously reported that mice injected with MFG-E8 showed symptoms of SLE-like autoimmune disease [16]. Here, we found that C2del induced autoantibody production in mice at a lower dose than wild-type MFG-E8. Since the half-life of C2del in the blood circulation was longer than that of the wild-type protein, it could have interfered more than wild-type with the phosphatidylserine-dependent phagocytosis of apoptotic cells. The same

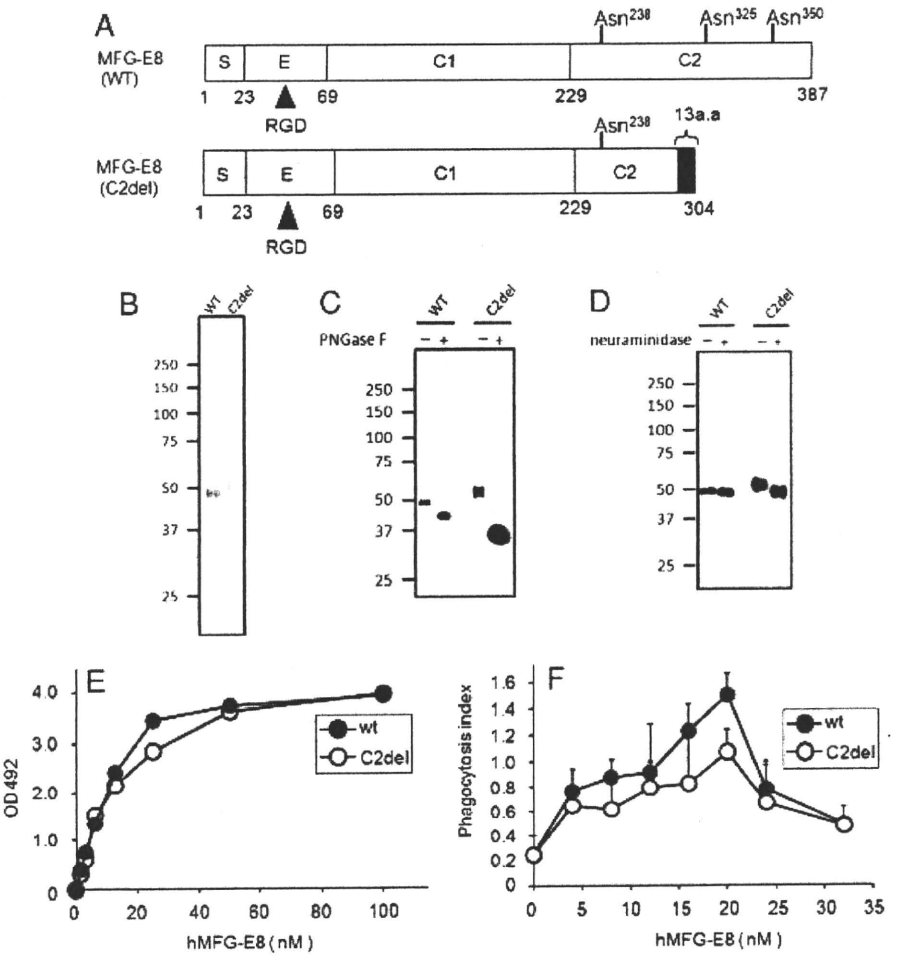

Figure 3. C2del binding to phosphatidylserine, and C2del-dependent phagocytosis of apoptotic cells. (A) Structure of the C2del mutant. C2del was truncated at the C2-homologous domain. Potential *N*-linked glycosylation sites (Asn^{238}, Asn^{325}, and Asn^{350}) are indicated. An extra 13-amino-acid region at the C-terminus of C2del is indicated as a filled box. S, Signal sequence; E, EGF domain; C1 and C2, Factor VIII-homologous domains; RGD, an Arg-Gly-Asp motif. (B) Preparation of human rMFG-E8. Purified wild-type and C2del MFG-E8 were analyzed by 10% SDS-PAGE and stained with Coomassie brilliant blue. (C) PNGase F treatment. Flag-tagged wild-type or C2del MFG-E8 was subjected to 10% SDS-PAGE before (–) or after (+) PNGase F treatment, and analyzed by Western blotting with an anti-Flag mAb. (D) Neuraminidase treatment. Flag-tagged wild-type or C2del MFG-E8 was subjected to 10% SDS-PAGE before (–) or after (+) neuraminidase digestion, and analyzed by Western blotting with the anti-Flag mAb. (E) Human MFG-E8 binding to phosphatidylserine. The indicated concentrations of wild-type MFG-E8 (•) or C2del (○) were added to a phosphatidylserine-coated microtiter plate. Bound proteins were detected by the anti-Flag mAb. Experiments were done in duplicate, and the mean values are shown. The experiments were done twice, and the representative data are shown. (F) Effect of human MFG-E8 on the phagocytosis of apoptotic cells. Apoptotic thymocytes (2×10^5 cells) were added to NIH3T3 transformants (1×10^4 cells) expressing integrin $\alpha_v\beta_3$ and incubated for 2 h with the indicated concentrations of wild-type MFG-E8 (•) or C2del (○). The cells were TUNEL-stained, and the phagocytosis index is expressed as the number of TUNEL-positive cells *per* phagocyte. The number of TUNEL-positive cells *per* phagocyte were determined for six fields that contain 20–30 phagocytes and is expressed as the phagocytosis index with SD. Data are representative of two independent experiments.

situation may apply in the patient, and the IVS 6-937 A>G mutation in the MFG-E8 gene may be a susceptibility mutation for SLE.

A recent SNP analysis of about 150 SLE patients in Taiwan indicated the predisposition of a specific SNP, causing a replacement of leucine to methionine at the amino acid position of 76 in the MFG-E8 gene, to SLE [34]. Here, we found two out of 322 SLE female patients carry a heterozygous intronic mutation that causes production of aberrant MFG-E8, and detected an aberrantly spliced MFG-E8 mRNA in mononuclear cells of the patient. Since MFG-E8 is mainly produced by Mac-1^+ cells in the immune system, we assume the aberrant MFG-E8 mRNA is produced from monocytes of the patients. In any case, whichever cells produce the aberrant form of the MFG-E8, it can cause SLE-type autoimmune disease. Splicing can be affected not only by *cis*-elements on the chromosomal gene but also by factors that regulate the splicing [35]. The presence of a cryptic exon in the MFG-E8 gene suggests that abnormal deviation in the splicing mechanism for the MFG-E8 gene can lead to the production of aberrant MFG-E8 protein. To elucidate the involvement of MFG-E8 in SLE pathogenesis in more detail, it will be necessary to analyze

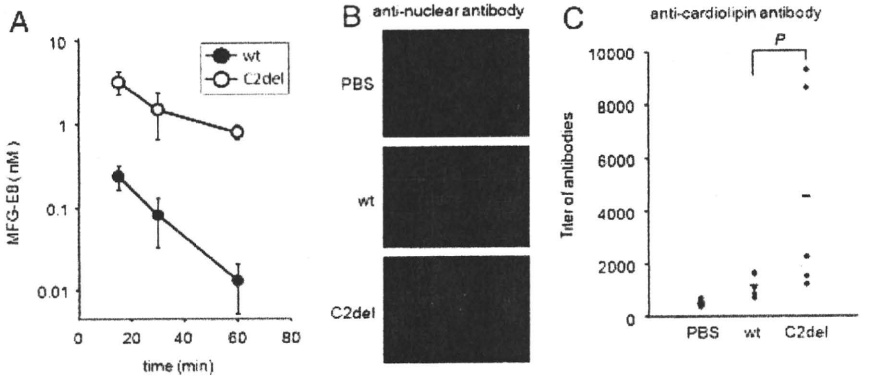

Figure 4. Production of autoantibodies in mice by C2del. (A) Clearance of human MFG-E8 from the blood circulation. Four mice were injected intravenously with 12 pmol of wild-type human MFG-E8 (●) or C2del (○), and bled at the indicated time points. The concentration of human MFG-E8 in serum was measured by an indirect ELISA as described in the *Materials and methods*. The mean concentrations are plotted with SD. (B) Detection of anti-nuclear antibodies by immunofluorescence on HEp-2. Five C57BL/6 female mice were injected intravenously with 12 pmol of wild-type or C2del weekly for four times. Blood samples were obtained 2 wk after the last injection. Human HEp-2 cells were incubated with 50-times diluted serum, and the antibodies bound to the cells were detected by Cy3-cojugated $F(ab')_2$ of goat anti-mouse IgG. All five mice gave a similar result, and representative results are shown. (C) Titer of anti-cardiolipin antibody. Five C57BL/6 female mice were injected intravenously with 12 pmol of wild-type or C2del weekly for six times. Blood samples were obtained 1 wk after the last injection, and the titer for anti-cardiolipin antibody was determined by ELISA as described in the *Materials and methods*. Average values obtained with five mice are indicated by horizontal bars. *p*-value, determined by Mann–Whitney's U-test, was 0.095.

comprehensively the MFG-E8 gene and its expression mechanism.

Materials and methods

Subjects

Blood mononuclear cells were collected from 110 female SLE patients at Nara Medical University Hospital, and 212 female SLE patients at Kyoto University Hospital. All the patients gave written informed consent. The ethical committees of the Graduate School of Medicine, Osaka University, the Graduate School of Medicine, Kyoto University, and Nara Medical University Hospital approved our study. Genomic DNA and RNA were prepared from the blood mononuclear cells using Gentra Puregene Blood kit (Qiagen) and Isogen-LS (Nippon Gene), respectively, and cDNA was synthesized with random hexamer as a primer.

Direct sequencing of the human MFG-E8 cDNA and chromosomal gene

The human MFG-E8 cDNA was amplified by PCR using the following two sets of primers: Ex1-S (5′-GTCTGAGCAGCCCAGCGT-3′) and Ex5-AS (5′-AGAGTGCAGGCCGTGTGGCA-3′); and Ex4-S (5′-GAACCTGCTGCGGAGGATGT-3′) and Ex8-AS (5′-GGCCCATGGAAAGCAGGAAG-3′). The PCR products were purified with a NucleoFast 96 PCR Plate (Macherey-Nagel). Cycle sequencing was performed using a BigDye Terminator v3.1 Cycle Sequencing kit and ABI 3100 genetic analyzer (Applied Biosystems). For sequencing the intron 6 of the MFG-E8 chromosomal gene, a DNA fragment was amplified by PCR using the following primers: (GGGACCTCTCCCTTGAGCAC and CCAGTTCGCACTGTCATTAC), and subjected to the cycle sequencing.

Splicing assay with a minigene

The normal and mutant (IVS 6-937) alleles of intron 6 in the human MFG-E8 gene were amplified from the genomic DNA of the SLE patient. The 1791 bp PstI-ApaI fragment carrying intron 6 was used to replace part (52 bp of PstI-ApaI DNA fragment) of the human MFG-E8 cDNA in pEF-BOS-hMFG-E8-Flag [15], and the product was verified by DNA sequencing. The minigene was introduced into HEp-2 cells by lipofection using Fugene 6 (Roche). Briefly, 1×10^5 cells were transfected with 0.5 μg DNA and cultured overnight in DMEM containing 10% FCS. After treating the cells for 2 h with 100 μg/mL cycloheximide, the total RNA was extracted from the cells using an RNeasy Mini Kit (Qiagen). The cDNA was synthesized with high capacity RNA-to-cDNA kit (Applied Biosystems) and subjected to PCR with the following primers: Cry-S, 5′-GCAGGACGATGATCTGCCTA-3′; Ex7-S, 5′-CGTAACTTTGGCTCTGTCCA-3′; and Flag-AS 5′-CGTCCTTGTAGTCGCTAGCA-3′.

Human rMFG-E8, binding to phosphatidylserine, and phagocytosis assay

To prepare human rMFG-E8, the cDNA for the Flag-tagged human MFG-E8 was inserted into pTRE2 expression vector (Clontech), and introduced into HAM3 cells, a HeLa tet-on cell

line [36], with a vector carrying the hygromycin-resistance gene. After selection with 0.5 mg/mL hygromycin, the transformant clones that produced MFG-E8 in a doxycycline-induced manner were selected. To produce MFG-E8, the transformants were treated with 1 μg/mL doxycycline in DMEM containing 1% FCS, and the secreted MFG-E8 was purified using anti-Flag M2 affinity gel (Sigma-Aldrich). To analyze the sugar moiety attached to human MFG-E8, rMFG-E8 (35 ng protein) was incubated at 37°C for 1 h with 0.1 unit of neuraminidase (Nacalai) or 500 units of PNGase F (New England Biolabs) and subjected to 10% SDS-PAGE, followed by Western blotting using an anti-Flag mAb.

The binding of hMFG-E8 to phosphatidylserine was determined by the solid-phase ELISA as described [20]. The Biacore technology using BiacoreX (GE Healthcare) with a HPA sensor chip was utilized to determine the dissociation constant for the binding of hMFG-E8 to phosphatidylserine according to Saenko *et al.* [37].

Phagocytosis was assayed as described previously [7] with NIH3T3 cell transformants expressing $\alpha_v\beta_3$ integrin as phagocytes and apoptotic CAD$^{-/-}$ thymocytes as preys. After engulfment, the cells were stained with TUNEL using an ApopTag peroxidase *in situ* apoptosis detection kit (Chemicon). The phagocytosis index was determined as the number of TUNEL-positive cells *per* phagocyte.

Injection of recombinant proteins

All animal experiments were carried out in accordance with protocols approved by the Animal Care and Use Committee of the Kyoto University Graduate School of Medicine. Human rMFG-E8 (12 pmol in 300 μL of PBS containing 2.5% serum from C57BL/6 mice) was intravenously administered into 8-wk-old C57BL/6 female mice through the tail vein. Serum was harvested 15, 30, and 60 min after the injection, and the MFG-E8 level was measured by an indirect sandwich ELISA. In brief, a 96-well Maxisorp plate (Nalge Nunc International) was coated with 1 μg/well of anti-FLAG mAb in 50 mM sodium bicarbonate buffer (pH 9.6) and incubated with Reagent Diluent Concentrate 2 (R&D Systems). Triton X-100 was added to the serum samples at a final concentration of 1%, the samples were diluted ten times with TBS, and a 50-μL aliquot was applied to each well. After a 1-h incubation, the wells were washed with wash buffer supplied with the Ampli Q kit (Dako), incubated with 0.8 μg/mL biotinylated hamster mAb against human MFG-E8 (clone 2–8E4A)[15], washed as above, and incubated with 8000-times-diluted alkaline phosphatase-conjugated streptavidin (Dako) for 30 min. The alkaline phosphatase activity was measured using the Ampli Q kit. Human rMFG-E8 diluted with 10% normal mouse serum was used to prepare the standard curve.

Detection of autoantibodies

C57BL/6 female mice at the age of 10 wk were treated weekly with 12 pmol of hMFG-E8 for a total of four or six times, and sera were collected before, and 6 and 7 wk after the first injection. The concentration of anti-cardiolipin antibody in the sera was measured by ELISA. In brief, 1 μg of cardiolipin in 100 μL of methanol was added to a 96-well plate (Immulon 1B microtiter plate; Thermo Labsystems), and the plate was air-dried. After blocking with 10% FCS, serially diluted mouse serum was added to the wells. After a 1-h incubation at room temperature, the mouse antibodies bound to the plate were detected using HRP-conjugated goat anti-mouse Ig (Dako) and peroxidase-detecting kit (Sumitomo Bakelite). The color reaction was read at 492 nm using a microplate reader (Titertek Instruments), and the titer of the antibody was defined as the dilution that gave the absorbance of 0.1.

Anti-nuclear antibody was detected by indirect immunofluorescence. In brief, human HEp-2 cells cultured on a glass slide were fixed with cold acetone and incubated with 50-times-diluted mouse serum at 37°C for 30 min. The antibodies bound to the HEp-2 cells were detected by Cy3-conjugated F(ab')$_2$ of goat anti-mouse IgG (Jackson ImmunoResearch Laboratories) diluted 100 times with PBS/10% normal goat serum, and observed by fluorescence microscopy (Biorevo, Keyence).

Acknowledgements: The authors thank M. Fujii and M. Harayama for secretarial assistance. This work was supported in part by Grants-in-Aid for Specially Promoted Research from the Ministry of Education, Science, Sports, and Culture in Japan to S. N. H. Y. was a Research Assistant for Osaka University Global COE program (System Dynamics of Biological Function).

Conflict of interest: The authors declare no financial or commercial conflict of interest.

References

1 **Adams, J. M.**, Ways of dying: multiple pathways to apoptosis. *Genes Dev.* 2003. **17**: 2481–2495.

2 **Fischer, U., Janicke, R. U. and Schulze-Osthoff, K.**, Many cuts to ruin: a comprehensive update of caspase substrates. *Cell Death Differ.* 2003. **10**: 76–100.

3 **Fadok, V. A., Bratton, D. L., Frasch, S. C., Warner, M. L. and Henson, P. M.**, The role of phosphatidylserine in recognition of apoptotic cells by phagocytes. *Cell Death Differ.* 1998. **5**: 551–562.

4 **Park, D., Tosello-Trampont, A. C., Elliott, M. R., Lu, M., Haney, L. B., Ma, Z., Klibanov, A. L. et al.**, BAI1 is an engulfment receptor for apoptotic cells upstream of the ELMO/Dock180/Rac module. *Nature* 2007. **450**: 430–434.

5 **Park, S. Y., Jung, M. Y., Kim, H. J., Lee, S. J., Kim, S. Y., Lee, B. H., Kwon, T. H. et al.**, Rapid cell corpse clearance by stabilin-2, a membrane phosphatidylserine receptor. *Cell Death Differ.* 2008. **15**: 192–201.

6 **Miyanishi, M., Tada, K., Koike, M., Uchiyama, Y., Kitamura, T. and Nagata, S.**, Identification of Tim4 as a phosphatidylserine receptor. *Nature* 2007. **450**: 435–439.

7 **Hanayama, R., Tanaka, M., Miwa, K., Shinohara, A., Iwamatsu, A. and Nagata, S.**, Identification of a factor that links apoptotic cells to phagocytes. *Nature* 2002. **417**: 182–187.

8 **D'Cruz, D. P., Khamashta, M. A. and Hughes, G. R.,** Systemic lupus erythematosus. *Lancet* 2007. **369**: 587–596.

9 **Gaipl, U. S., Voll, R. E., Sheriff, A., Franz, S., Kalden, J. R. and Herrmann, M.,** Impaired clearance of dying cells in systemic lupus erythematosus. *Autoimmun. Rev.* 2005. **4**: 189–194.

10 **Steinman, C. R.,** Circulating DNA in systemic lupus erythematosus. Isolation and characterization. *J. Clin. Invest.* 1984. **73**: 832–841.

11 **Rumore, P. M. and Steinman, C. R.,** Endogenous circulating DNA in systemic lupus erythematosus. Occurrence as multimeric complexes bound to histone. *J. Clin. Invest.* 1990. **86**: 69–74.

12 **Raymond, A., Ensslin, M. A. and Shur, B. D.,** SED1/MFG-E8: a bi-motif protein that orchestrates diverse cellular interactions. *J. Cell Biochem.* 2009. **106**: 957–966.

13 **Miyasaka, K., Hanayama, R., Tanaka, M. and Nagata, S.,** Expression of milk fat globule epidermal growth factor 8 in immature dendritic cells for engulfment of apoptotic cells. *Eur. J. Immunol.* 2004. **34**: 1414–1422.

14 **Hanayama, R., Tanaka, M., Miyasaka, K., Aozasa, K., Koike, M., Uchiyama, Y. and Nagata, S.,** Autoimmune disease and impaired uptake of apoptotic cells in MFG-E8-deficient mice. *Science* 2004. **304**: 1147–1150.

15 **Yamaguchi, H., Takagi, J., Miyamae, T., Yokota, S., Fujimoto, T., Nakamura, S., Ohshima,S. *et al.*,** Milk fat globule EGF factor 8 in the serum of human patients of systemic lupus erythematosus. *J. Leukoc. Biol.* 2008. **83**: 1300–1307.

16 **Asano, K., Miwa, M., Miwa, K., Hanayama, R., Nagase, H., Nagata, S. and Tanaka, M.,** Masking of phosphatidylserine inhibits apoptotic cell engulfment and induces autoantibody production in mice. *J. Exp. Med.* 2004. **200**: 459–467.

17 **Wang, Z. and Burge, C. B.,** Splicing regulation: from a parts list of regulatory elements to an integrated splicing code. *RNA* 2008. **14**: 802–813.

18 **Hertel, K. J.,** Combinatorial control of exon recognition. *J. Biol. Chem.* 2008. **283**: 1211–1215.

19 **Mizushima, S. and Nagata, S.,** pEF-BOS, a powerful mammalian expression vector. *Nucleic Acids Res.* 1990. **18**: 5322.

20 **Andersen, M. H., Berglund, L., Rasmussen, J. T. and Petersen, T. E.,** Bovine PAS-6/7 binds $\alpha_v\beta_5$ integrins and anionic phospholipids through two domains. *Biochemistry* 1997. **36**: 5441–5446.

21 **Gregoriadis, G., Jain, S., Papaioannou, I., Laing, P.,** Improving the therapeutic efficacy of peptides and proteins: a role for polysialic acids. *Int. J. Pharm.* 2005. **300**: 125–130.

22 **Chitlaru, T., Kronman, C., Zeevi,M., Kam, M., Harel, A., Ordentlich, A., Velan, B. and Shafferman, A.,** Modulation of circulatory residence of recombinant acetylcholinesterase through biochemical or genetic manipulation of sialylation levels. *Biochem. J.* 1998. **336**: 647–658.

23 **Johnson, J. M., Castle, J., Garrett-Engele, P., Kan, Z., Loerch, P. M., Armour, C. D., Santos,R. *et al.*,** Genome-wide survey of human alternative pre-mRNA splicing with exon junction microarrays. *Science* 2003. **302**: 2141–2144.

24 **Wang, G. S. and Cooper, T. A.,** Splicing in disease: disruption of the splicing code and the decoding machinery. *Nat. Rev. Genet.* 2007. **8**: 749–761.

25 **McCullough, A. J. and Berget, S. M.,** G triplets located throughout a class of small vertebrate introns enforce intron borders and regulate splice site selection. *Mol. Cell. Biol.* 1997. **17**: 4562–4571.

26 **Yeo, G., Hoon, S., Venkatesh, B. and Burge, C. B.,** Variation in sequence and organization of splicing regulatory elements in vertebrate genes. *Proc. Natl. Acad. Sci. USA* 2004. **101**: 15700–15705.

27 **Chou, M. Y., Rooke, N., Turck, C. W. and Black, D. L.,** hnRNP H is a component of a splicing enhancer complex that activates a c-src alternative exon in neuronal cells. *Mol. Cell. Biol.* 1999. **19**: 69–77.

28 **McCullough, A. J. and Berget, S. M.,** An intronic splicing enhancer binds U1 snRNPs to enhance splicing and select 5′ splice sites. *Mol. Cell. Biol.* 2000. **20**: 9225–9235.

29 **Wen, J. and Brogna, S.,** Nonsense-mediated mRNA decay. *Biochem. Soc. Trans.* 2008. **36**: 514–516.

30 **Bateman, J. F., Freddi, S., Nattrass, G. and Savarirayan, R.,** Tissue-specific RNA surveillance? Nonsense-mediated mRNA decay causes collagen X haploinsufficiency in Schmid metaphyseal chondrodysplasia cartilage. *Hum. Mol. Genet.* 2003. **12**: 217–225.

31 **Kerr, T. P., Sewry, C. A., Robb, S. A. and Roberts, R. G.,** Long mutant dystrophins and variable phenotypes: evasion of nonsense-mediated decay? *Hum. Genet.* 2001. **109**: 402–407.

32 **Morrissette, J. D., Colliton, R. P. and Spinner, N. B.,** Defective intracellular transport and processing of JAG1 missense mutations in Alagille syndrome. *Hum. Mol. Genet.* 2001. **10**: 405–413.

33 **Cheng, S. H., Gregory, R. J., Marshall, J., Paul, S., Souza, D. W., White, G. A., O'Riordan, C. R. and Smith, A. E.,** Defective intracellular transport and processing of CFTR is the molecular basis of most cystic fibrosis. *Cell* 1990. **63**: 827–834.

34 **Hu, C., Wu, C., Tsai, H., Chang, S., Tsai, W. and Hsu, P.,** Genetic polymorphism in milk fat globule-EGF factor 8 (MFG-E8) is associated with systemic lupus erythematosus in human. *Lupus* 2009. **18**: 676–681.

35 **Chen, M. and Manley, J. L.,** Mechanisms of alternative splicing regulation: insights from molecular and genomics approaches. *Nat. Rev. Mol. Cell Biol.* 2009. **10**: 741–754.

36 **Watanabe-Fukunaga, R., Iida, S., Shimizu, Y., Nagata, S. and Fukunaga, R.,** SEI family of nuclear factors regulates p53-dependent transcriptional activation. *Genes Cells* 2005. **10**: 851–860.

37 **Saenko, E., Sarafanov, A., Ananyeva, N., Behre, E., Shima, M., Schwinn, H. and Josic, D.,** Comparison of the properties of phospholipid surfaces formed on HPA and L1 biosensor chips for the binding of the coagulation factor VIII. *J. Chromatogr. A* 2001. **921**: 49–56.

38 **Kawane, K., Fukuyama, H., Yoshida, H., Nagase,H., Ohsawa, Y., Uchiyama, Y., Iida, T. *et al.*,** Impaired thymic development in mouse embryos deficient in apoptotic DNA degradation. *Nat. Immunol.* 2003. **4**: 138–144.

Abbreviations: **MFG-E8:** milk fat globule-EGF factor 8 · **NMD:** nonsense-mediated mRNA decay · **SLE:** systemic lupus erythematosus

Full correspondence: Professor Shigekazu Nagata, Department of Medical Chemistry, Graduate School of Medicine, Kyoto University, Yoshida-Konoe, Sakyo, Kyoto 606-8501, Japan
Fax: +81-75-753-9446
e-mail: snagata@mfour.med.kyoto-u.ac.jp

Current address: Shinobu Nakamura, Medical Corporation Katsurakai Hirao Hospital, 6-28 Hyobu, Kashihara, Nara 634-0076, Japan

Received: 27/10/2009
Revised: 5/2/2010
Accepted: 25/2/2010
Accepted article online: 8/3/2010

ARTHRITIS & RHEUMATISM
Vol. 62, No. 10, October 2010, pp 2963–2972
DOI 10.1002/art.27590

Protective Targeting of High Mobility Group Box Chromosomal Protein 1 in a Spontaneous Arthritis Model

Therese Östberg,[1] Kohki Kawane,[2] Shigekazu Nagata,[2] Huan Yang,[3] Sangeeta Chavan,[3] Lena Klevenvall,[1] Marco E. Bianchi,[4] Helena Erlandsson Harris,[1] Ulf Andersson,[1] and Karin Palmblad[1]

Objective. **High mobility group box chromosomal protein 1 (HMGB-1) is a DNA binding nuclear protein that can be released from dying cells and activated myeloid cells. Extracellularly, HMGB-1 promotes inflammation. Clinical and experimental studies demonstrate that HMGB-1 is a pathogenic factor in chronic arthritis. Mice with combined gene deficiency for *DNase II* and *IFNRI* spontaneously develop chronic, destructive polyarthritis with many features shared with rheumatoid arthritis. DNase II is needed for macrophage degradation of engulfed DNA. The aim of this study was to evaluate a potential pathogenic role of HMGB-1 in this novel murine model.**

Methods. **The course of arthritis, assessed by clinical scoring and histology, was studied in *DNase II*$^{-/-}$ × *IFNRI*$^{-/-}$ mice, in comparison with heterozygous and wild-type mice. Synovial HMGB-1 expression was analyzed by immunohistochemistry. Serum levels of HMGB-1 were determined by Western immunoblotting and enzyme-linked immunosorbent assay (ELISA), and anti–HMGB-1 autoantibodies were detected by ELISA. Macrophage activation was studied by immunostaining for intracellular interleukin-1β and HMGB-1. HMGB-1 was targeted with truncated HMGB-1–derived BoxA protein, acting as a competitive antagonist, with intraperitoneal injections every second day for 5 weeks.**

Results. ***DNase II*$^{-/-}$ × *IFNRI*$^{-/-}$ **mice developed symmetric polyarthritis with strong aberrant cytosolic and extracellular HMGB-1 expression in synovial tissue, in contrast to that observed in control animals. Increased serum levels of HMGB-1 and HMGB-1 autoantibodies were recorded in *DNase II*$^{-/-}$ × *IFNRI*$^{-/-}$ mice, both prior to and during the establishment of disease. Systemic HMGB-1–specific blockade significantly ameliorated the clinical disease course, and a protective effect on joint destruction was demonstrated by histologic evaluation.**

Conclusion. **HMGB-1 is involved in the pathogenesis of this spontaneous polyarthritis, and intervention with an HMGB-1 antagonist can mediate beneficial effects.**

There are several experimental animal models of rheumatoid arthritis (RA), each with advantages and shortcomings when compared with the human disease (for review, see ref. 1). A novel experimental arthritis model was recently described, in which mice with double-gene deficiency for *DNase II* and *IFNRI* (the gene for type I interferon [IFN] receptor) spontaneously develop destructive chronic polyarthritis (2). These mice have a severely reduced macrophage capacity to degrade DNA of the engulfed apoptotic cells and expelled erythroid cell nuclei. A large pool of chromosomal DNA is generated during erythropoiesis, and programmed cell death and the presence of DNase II in macrophages are

Supported by the Stockholm County Council and Karolinska Institutet through a regional agreement on medical training and clinical research (*ALF*), the Swedish Association Against Rheumatism, the Swedish Medical Research Council, the Åke Wiberg Foundation, Stiftelsen Allmänna Barnhuset, the Freemason Lodge Barnhuset in Stockholm, and the King Gustaf V Memorial Foundation.

[1]Therese Östberg, PhD, Lena Klevenvall, BSci, Helena Erlandsson Harris, PhD, Ulf Andersson, MD, PhD, Karin Palmblad, MD, PhD: Astrid Lindgren Children's Hospital, Karolinska Hospital, and Karolinska Institutet, Stockholm, Sweden; [2]Kohki Kawane, PhD, Shigekazu Nagata, MD, PhD: Kyoto University, Kyoto, Japan; [3]Huan Yang, PhD, Sangeeta Chavan, PhD: Feinstein Institute for Medical Research, North Shore–Long Island Jewish Health System, Manhasset, New York; [4]Marco E. Bianchi, MD, PhD: San Raffaele Scientific Institute, Milan, Italy.

Dr. Bianchi is part owner of HMGBiotech Srl.

Address correspondence and reprint requests to Karin Palmblad, MD, PhD, Department of Women's and Children's Health, Pediatric Rheumatology Research Unit, Karolinska Institutet/Karolinska University Hospital, Stockholm, Sweden. E-mail: Karin.Palmblad@ki.se.

Submitted for publication February 4, 2010; accepted in revised form May 25, 2010.

specifically required for digestion of the lysosomal DNA after engulfment (3). However, *DNase II*$^{-/-}$ mice die as embryos, due to an as yet unexplained potent constitutive production of IFNβ (4), but lethality is prevented by silencing the *IFNRI* gene, thereby impeding IFNβ as well as IFNα signaling (5).

DNase II$^{-/-}$ × *IFNRI*$^{-/-}$ mice are born without a distinct phenotype but then spontaneously develop a clinical disease resembling human RA at the age of ~2 months. Symmetric polyarthritis initially affecting the digits is followed by arthritis in larger joints. Histologic analyses of the affected joints have revealed synovitis with villus proliferation, accompanied by pannus formation and eroded joint anatomy. Sera from *DNase II*$^{-/-}$ × *IFNRI*$^{-/-}$ mice contain high levels of anti–cyclic citrullinated peptide antibodies, rheumatoid factor, and matrix metalloproteinase 3. Cytokines known to be highly expressed in the joints of patients with RA, such as tumor necrosis factor (TNF), interleukin-1β (IL-1β), IL-6, IL-10, and IL-18, are also detectable. Furthermore, therapeutic administration of anti-TNF antibodies ameliorates arthritis in this model (2). The macrophage activation is central in disease pathogenesis. Since mammalian DNA is a poor proinflammatory mediator, we considered the possibility that molecules, such as high mobility group box chromosomal protein 1 (HMGB-1), that are attached to the undigested chromatin may be involved in the process.

HMGB-1 is a nonhistone DNA-binding nuclear protein that displays both intracellular and extracellular activities. In the nucleus, HMGB-1 binds and bends the chromatin and regulates transcription, interacting with both DNA and transcription factors (6,7). The intracellular location of HMGB-1 is, however, not fixed, and, depending on the state of the cell, HMGB-1 can transit to the extracellular space to activate innate immunity. The translocation of HMGB-1 from the inside to the outside of the cell is thus a critical event in inflammation and host defense, and can occur via 2 separate mechanisms. Stimulated inflammatory cells, including macrophages, may, through a regulated process, actively secrete HMGB-1 (8–11). In addition, HMGB-1 can also be passively released during disintegration of primary necrotic cells or apoptotic bodies undergoing secondary necrosis (12,13).

During the past decade, the widespread use of antagonists that neutralize HMGB-1 in standardized preclinical studies of disease has directly implicated a pathogenic role of this molecule in arthritis, colitis, sterile ischemia, traumatic injury, cancer, and infection (14–19). Key observations connecting HMGB-1 to arthritis include the following: 1) therapeutic targeting of HMGB-1 using antagonistic, truncated HMGB-1 BoxA protein or neutralizing HMGB-1–specific antibodies has been shown to prevent progression of arthritis in animals and, in particular, ameliorates structural damage (for review, see ref. 20); 2) HMGB-1 is released at the site of joint inflammation, and tissue specimens from RA patients with synovitis reveal aberrant HMGB-1 expression, particularly in areas where synovial tissue invades cartilage and bone (21,22); 3) hypoxic areas in synovitis colocalize with aberrant HMGB-1 expression (23); 4) injection of HMGB-1 into normal animal joints causes destructive arthritis (24); 5) HMGB-1 regulates the production of, and acts upstream of, TNF, IL-1β, IL-6, and tissue-degrading proteinases (25–27); and 6) HMGB-1 plays a pivotal role in the maturation of osteoclasts (28–30). In the present study, we investigated the potential role of HMGB-1 in a novel murine arthritis model that recapitulates important features of human RA.

MATERIALS AND METHODS

Mice. Mice deficient in the *DNase II* and *IFNRI* genes were generated as described previously (5). Because of impaired fertility in *DNase II*$^{-/-}$ × *IFNRI*$^{-/-}$ mice, heterozygous *DNase II*$^{+/-}$ × *IFNRI*$^{-/-}$ mice were kept for breeding. Animals were housed in specific pathogen–free facilities at Karolinska University Hospital. All experiments were approved by the Stockholm North Ethical Committee. The mice had free access to water and standard rodent chow. A 12-hour light/dark circle was maintained at all times.

For determination of the *DNase II* genotypes, genomic DNA was prepared from ear biopsy tissue for detection of the *DNase II*–null allele by polymerase chain reaction. Mice were observed for clinical signs of arthritis, such as erythema and swelling of the joints. The interphalangeal joints of the digits, metacarpal joints, and wrists in the fore paw and in the metatarsal and ankle joints in the hind paw were each considered as one category of joint. Individual paws were evaluated using a clinical arthritis score ranging from 0 to 3, in which 0 = no signs of arthritis, 1 = one type of joint affected, 2 = two types of joints affected, and 3 = the entire paw affected, including signs of ankylosis. Thus, the maximal score for each animal was 12. Evaluation of arthritis was performed by staff members (TÖ, LK, and KP) who were blinded with regard to the identity of the animals.

Prophylactic intervention with BoxA protein, an HMGB-1 antagonist. At the age of 6 weeks, 1–2 weeks before the expected onset of clinical disease, therapy was initiated and animals (n = 7) were injected intraperitoneally with 400 μg of BoxA, an HMGB-1 antagonist (HMGBiotech) every second day for a period of 5 weeks. Control animals (n = 8) received equal volumes of vehicle (phosphate buffered saline [PBS]) alone.

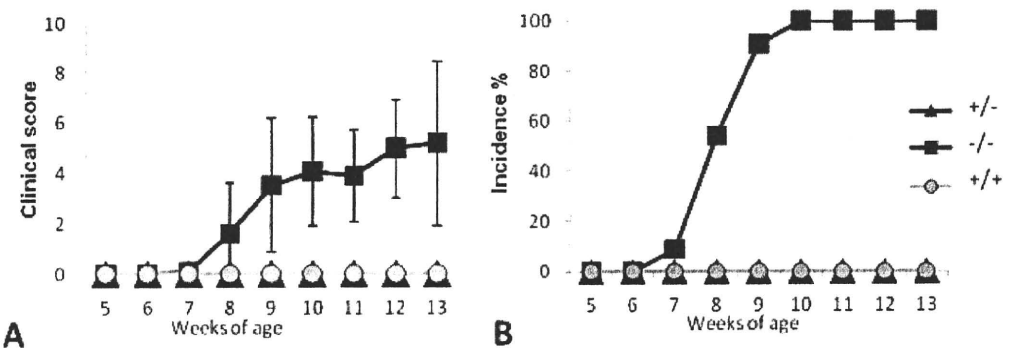

Figure 1. Clinical progression of arthritis. Mice were observed for clinical signs of arthritis and assigned an arthritis score with a maximal value of 12. *DNase II*$^{-/-}$ × *IFNRI*$^{-/-}$ mice spontaneously developed arthritis at ~7–8 weeks of age (**A**), with 100% incidence at 10 weeks of age (**B**), while heterozygous *DNase II*$^{+/-}$ × *IFNRI*$^{-/-}$and wild-type mice remained clinically healthy throughout the observation period. Bars show the mean ± SD.

Immunohistochemical staining of synovial and spleen specimens. Paws and spleens were collected, dissected, and fixed in 4% formaldehyde at 4°C overnight. Thereafter, the paws were decalcified in EDTA buffer for 3–4 weeks before dehydration and paraffin embedding. Immunohistochemical staining was performed on serial, paraffin-embedded 5-μm tissue sections. Slides were preheated at 60°C overnight before deparaffinization in xylene and rehydration with ethanol. Subsequently, antigen retrieval was achieved by microwave irradiation in 0.05% citraconic anhydride buffer, pH 7.4 (98%; Sigma-Aldrich). For detection of HMGB-1 expression, sections were stained according to protocols previously described (22). Briefly, to reduce background staining due to nonspecific binding, sections were incubated with Background Buster (Innovex Biosciences), and endogenous biotin was blocked with an avidin/biotin blocking kit (Vector Laboratories). Slides were incubated overnight with an affinity-purified monoclonal mouse IgG2b anti–HMGB-1 antibody (2G7, concentration 2 μg/ml; received as a hybridoma from Critical Therapeutics). A biotin-labeled goat anti-mouse IgG2b antibody (Caltag Laboratories) was used for detection. Stainings were developed using a diaminobenzidine kit (Vector Laboratories) according to the instructions of the manufacturer. Sections were counterstained with Mayer's hematoxylin (Histolab).

Assessment of joint pathologic features. Serial sections were stained with hematoxylin and eosin to evaluate synovial hyperplasia and inflammatory cell infiltration of the joints or with Safranin O (0.1%) to determine proteoglycan depletion, cartilage damage, and bone erosions. Cell infiltration and synovial hyperplasia were graded on a scale from 0 (no

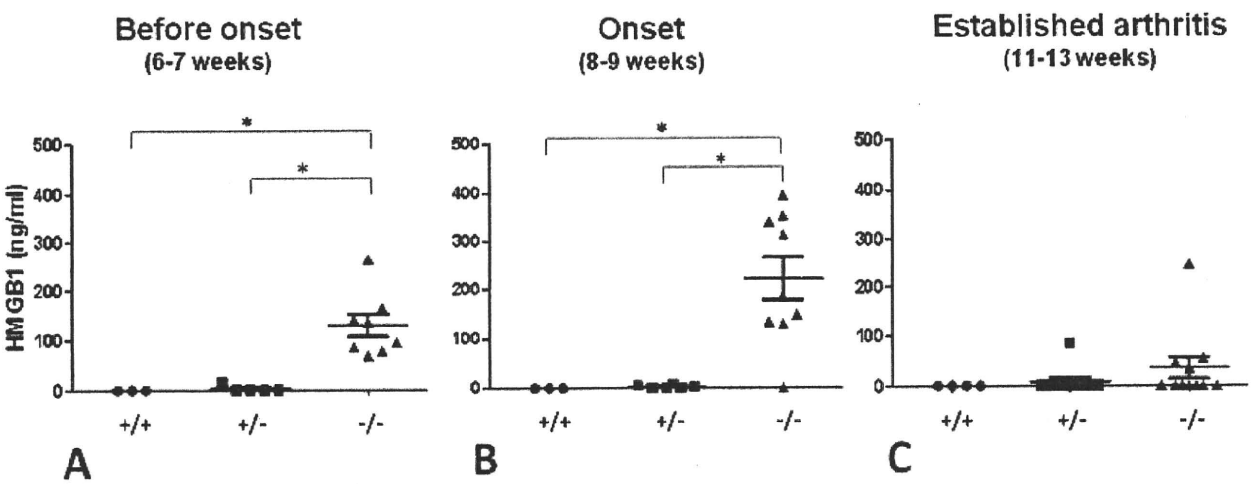

Figure 2. Presence of high mobility group box chromosomal protein 1 (HMGB-1) in mouse serum. HMGB-1 was readily detected in the sera of *DNase II*$^{-/-}$ × *IFNRI*$^{-/-}$ mice before the onset of arthritis (**A**), with peak release of HMGB-1 into the circulation occurring at arthritis onset (**B**). In established arthritis, serum levels of HMGB-1 subsided to levels that were not significantly different from those in age-matched heterozygous littermates and wild-type mice (**C**). Bars show the mean ± SD. * = $P < 0.05$.

infiltration/normal synovium) to 3 (severely inflamed joint with maximal cellular influx/synovial hyperplasia). Cartilage destruction and matrix proteoglycan depletion were scored on a scale of 0–3, ranging from no abnormalities (score 0) to completely destroyed or destained cartilage (score 3). Bone erosions were graded on a scale from 0 (normal bone appearance) to 3 (fully eroded cortical bone), using a grading scheme adapted from one previously described (31).

Immunocytochemical staining of peritoneal macrophages. Peritoneal macrophages were obtained from mice by intraperitoneal flushing with PBS. Cells were washed by centrifugation and transferred to 8-chamber culturing slides (BD Biosciences) at 50×10^3 cells/ml, and were allowed to adhere for 24 hours in Dulbecco's modified Eagle's medium (Gibco, Innovagen) supplemented with 5% fetal calf serum, before fixation with 4% formaldehyde. After washes in PBS, slides were blocked with 2% fetal calf serum, followed by blocking of endogenous biotin by an avidin/biotin blocking step. For detection of HMGB-1, the cells were incubated with the same antibody pair as for immunohistochemical staining. For detection of IL-1β, a primary goat anti–IL-1β antibody (AF-501-NA; R&D Systems) and a secondary biotinylated donkey anti-sheep/anti-goat antibody (The Binding Site) were used. The incubation times, lasting 2 hours for HMGB-1 and 30 minutes for IL-1β, were shorter than that required in the immunohistochemical staining protocol. Thereafter, cells were incubated with Alexa Fluor 488–conjugated avidin (Molecular Probes, Invitrogen) for 30 minutes, and nuclei were counterstained with Hoechst 33258.

For both immunohistochemical and immunocytochemical staining procedures, PBS supplemented with 0.1% saponin was used in all subsequent washes and incubation steps, in order to permeabilize the cells. In each assay, controls for staining specificity were included, based on parallel staining studies omitting the primary antibody and using a primary isotype-matched immunoglobulin of irrelevant antigen specificity (negative control mouse IgG2b; Dako Cytomation) and goat anti-human IL-2 (AF-202; R&D Systems). The specificities of intracellular HMGB-1 immunoreactivities were further verified by blocking experiments with preabsorption of the HMGB-1–specific antibody with recombinant HMGB-1 prior to staining.

Serologic analysis. Serum samples were collected for serologic analysis at 3 different time points: before arthritis onset (ages 6–7 weeks), at expected onset (ages 8–9 weeks), and at the time of established arthritis (ages 11–13 weeks), from individual *DNase II*$^{-/-}$ × *IFNRI*$^{-/-}$ mice (n = 11), as well as from age-matched heterozygous *DNase II*$^{+/-}$ × *IFNRI*$^{-/-}$ littermates (n = 10) and wild-type mice (n = 4). Serologic analyses were performed on coded serum samples, with the identity of the animals revealed only after results had been obtained.

HMGB-1 measurements. The presence of HMGB-1 in the serum was determined by Western immunoblotting, as described previously (32). Briefly, serum samples of 30–100 μl were ultrafiltered with Centricon 100 (Millipore). Serum was pooled when volumes were insufficient. The eluate was fractionated by 4–20% sodium dodecyl sulfate–polyacrylamide gel electrophoresis, transferred to a polyvinylidene difluoride immunoblot membrane (Bio-Rad), and probed with either specific anti–HMGB-1 antiserum (1:250 dilution) or purified IgG from anti–HMGB-1 antiserum (5 μg/ml) for Western blot analysis. Polyclonal anti–HMGB-1 rabbit IgG was purified using protein A–agarose (Pierce) according to the manufacturer's instructions. Western blots were scanned with a silver image scanner (Silver Scanner II; Lacie Limited), and the relative band intensity was quantified using NIH Image version 1.59 software. The levels of HMGB-1 were determined by reference to standard curves generated with purified HMGB-1. In addition, serum samples were assayed using an HMGB-1–specific enzyme-linked immunosorbent assay (ELISA) kit (Shino-Test Corporation).

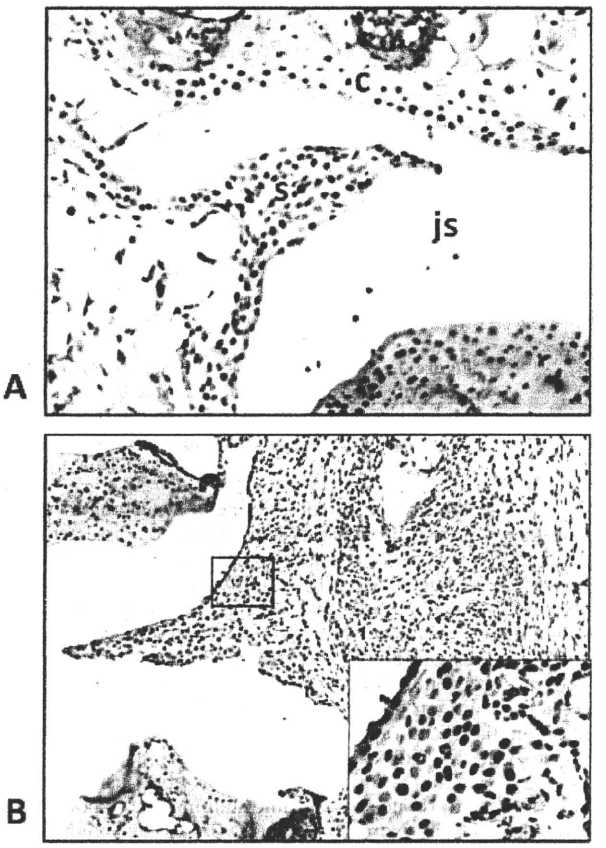

Figure 3. Expression of extranuclear high mobility group box chromosomal protein 1 (HMGB-1) protein in the arthritic joints of *DNase II* × *IFNRI*–deficient mice. Representative photomicrographs illustrate immunohistochemical staining with diaminobenzidine brown for HMGB-1 in paraffin-embedded paw sections. **A,** Nonarthritic lesions, before arthritis onset, in the paw tissue were characterized by predominantly nuclear HMGB-1 staining in the synovial membrane. **B,** Arthritic lesions, early after arthritis onset, showed abundant expression of HMGB-1 and nuclear, as well as cytosolic, expression of HMGB-1 and an additional extracellular presence of HMGB-1. **s** = synovial tissue; **js** = joint space; **c** = cartilage. (Original magnification × 125 in **A** and × 100 in **B; inset** shows a higher-magnification view [× 400] of the boxed area in **B.**)

Anti–HMGB-1 antibody ELISA. To determine the levels of autoantibodies, serum samples were analyzed with an

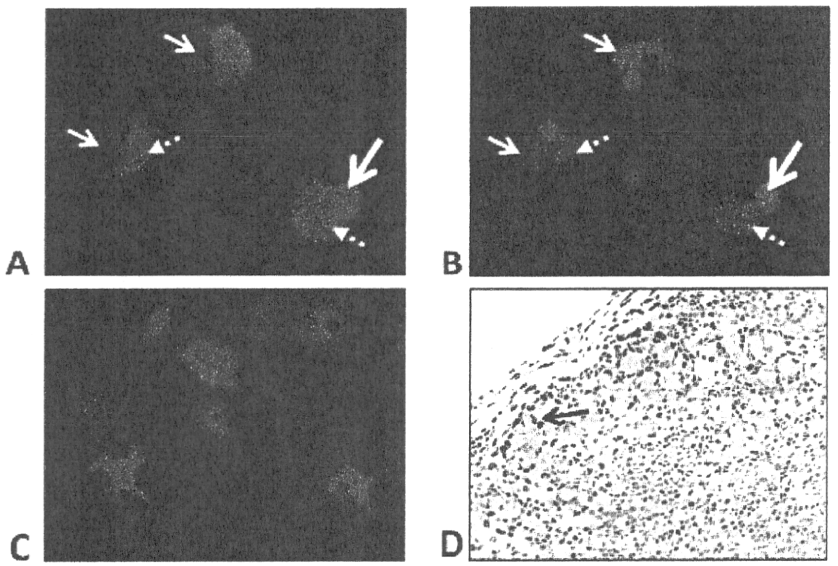

Figure 4. Cytoplasmic high mobility group box chromosomal protein 1 (HMGB-1) expression in abnormal macrophages. **A** and **B,** Representative photomicrographs illustrate peritoneal *DNase II*$^{-/-}$ × *IFNRI*$^{-/-}$ macrophages stained for HMGB-1 (with green Alexa Fluor 488). Intranuclear staining of HMGB-1 (**dotted arrows**) and additional HMGB-1 staining in the cytoplasm (**solid arrows**) are evident in the macrophages (**A**). Counterstaining with Hoechst 33258 reveals DNA in the cell nuclei (**dotted arrows**) and in undigested DNA (**solid arrows**) in multiple enlarged vacuoles in the cytoplasm (**B**). Some of the vacuoles containing undigested DNA also contain HMGB-1 (**large solid arrow**), although the majority are devoid of HMGB-1 (**small solid arrows**). **C,** A substantial portion of *DNase II*$^{-/-}$ × *IFNRI*$^{-/-}$ macrophages were found to express interleukin-1β, as a sign of macrophage activation. **D,** Immunostaining of a spleen tissue section (with diaminobenzidine brown) from a *DNase II*$^{-/-}$ × *IFNRI*$^{-/-}$ mouse demonstrates abundant nuclear, as well as extranuclear, HMGB-1 expression, while undigested DNA in the abnormal macrophages mostly appears devoid of HMGB-1 (**arrow**). (Original magnification × 800 in **A, B,** and **D;** × 125 in **C.**)

ELISA. Briefly, 96-well plates (Nunc MaxiSorp; Thermo Fisher Scientific) were coated with 5 μg/ml recombinant HMGB-1 produced in *Escherichia coli* and purified as previously described (32), with endotoxin levels determined to be below 0.03 EU/μg protein as measured using the Limulus assay. Sera diluted to 1:100 with Dulbecco's PBS (Gibco, Invitrogen) was added, followed by incubation for 2 hours at room temperature. Thereafter, horseradish peroxidase–conjugated anti-mouse IgG antibody, diluted 1:10,000, was added. Tetramethylbenzidine was added to develop the plate, and the reaction was stopped with 12.5% sulfuric acid. Absorbance was measured at 450 nm using a microplate reader (Multiscan MS TM; Labsystems).

Statistical analysis. Kruskal-Wallis nonparametric analysis of variance was used to compare levels of HMGB-1 and anti–HMGB-1 antibodies in the serum. All pairwise comparisons were adjusted using Dunn's multiple comparisons test. Linear regression was used when evaluating the extent to which there were associations between the frequencies of HMGB-1 and anti–HMGB-1 antibodies. The area under the curve was calculated for the effects of therapeutic intervention with BoxA, and differences between the groups were evaluated by unpaired *t*-test. *P* values less than 0.05 were considered significant. The software program GraphPad Prism version 5 for Windows (GraphPad Software) was used for all tests.

RESULTS

Development of polyarthritis in *DNase II* × *IFNRI*–deficient mice. The disease course was clinically evaluated daily in *DNase II*$^{-/-}$ × *IFNRI*$^{-/-}$ mice, in comparison with age-matched heterozygous *DNase II*$^{+/-}$ × *IFNRI*$^{-/-}$ mice and wild-type mice, using clinical scores of arthritis and accumulated incidence for 7 weeks starting from the age of 6 weeks. The majority of *DNase II*$^{-/-}$ × *IFNRI*$^{-/-}$ mice developed arthritis at ~7–8 weeks of age, with an incidence of 100% at 10 weeks of age (Figures 1A and B). Arthritis initially affected the digits, with subsequent involvement of

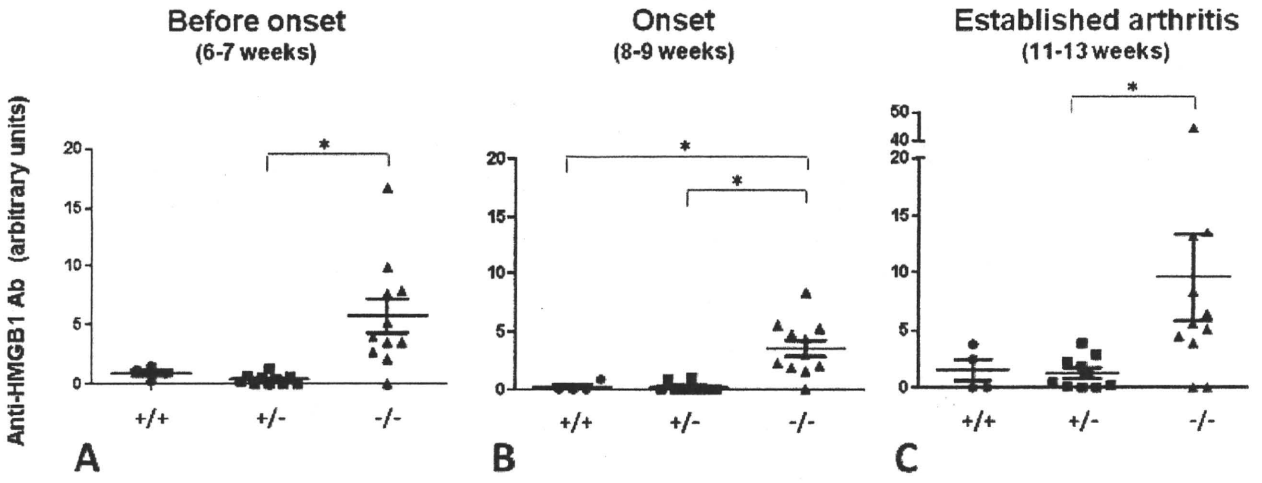

Figure 5. Serum analysis of anti–high mobility group box chromosomal protein 1 (anti–HMGB-1) autoantibodies (Ab) in *DNase II*$^{-/-}$ × *IFNRI*$^{-/-}$ mice, compared with age-matched heterozygous littermates and wild-type mice. HMGB-1 autoantibodies appeared before disease onset (**A**) in *DNase II*$^{-/-}$ × *IFNRI*$^{-/-}$ mice. Thereafter, the autoantibody levels were maintained at onset of arthritis (**B**) and then were found to be increased when recorded at the time of established arthritis (**C**) in *DNase II* × *IFNRI*–deficient mice. Bars show the mean ± SD. * = $P < 0.05$.

larger joints, including the wrists and ankles, and gradual loss of grip strength and, eventually, signs of joint deformation. Although heterozygous *DNase II*$^{+/-}$ × *IFNRI*$^{-/-}$ mice were clinically healthy, histologic evaluation of the articular specimens revealed signs of mild synovitis in a few of these mice. The majority of heterozygous mice and all of the wild-type mice remained healthy throughout the observation period, as characterized by normal joint histologic features.

Systemic expression of HMGB-1 in *DNase II* × *IFNRI*–deficient mice. HMGB-1 levels were measured by Western blot analyses in serum samples obtained at different time points. HMGB-1 was readily detected in the sera from all *DNase II*$^{-/-}$ × *IFNRI*$^{-/-}$ mice beginning at the earliest studied time point, before the onset of clinical disease (Figure 2A). The levels then increased significantly, with peak release of circulating HMGB-1 occurring at the onset of arthritis (Figure 2B). However, the serum HMGB-1 levels in established arthritis subsided to levels that were not significantly different from those in age-matched heterozygous littermates and wild-type mice (Figure 2C). These results were verified in an HMGB-1–specific ELISA (results not shown).

Expression of extranuclear HMGB-1 protein in the arthritic joints of *DNase II* × *IFNRI*–deficient mice. Immunohistochemical staining was performed to study the intracellular localization of HMGB-1 in the articular tissue of nonarthritic as well as arthritic *DNase II*$^{-/-}$ × *IFNRI*$^{-/-}$ mice, compared with that of control wild-type mice. The localization of HMGB-1 was predominantly intranuclear in sections from normal joints, in which only resident synovial cells were present, and there were no discernable differences between healthy *DNase II*$^{-/-}$ × *IFNRI*$^{-/-}$ mice and control mice (Figure 3A). No influx of inflammatory cells or abnormal macrophages could be visualized in nonarthritic *DNase II*$^{-/-}$ × *IFNRI*$^{-/-}$ mice. In contrast, joint tissue specimens from arthritic *DNase II*$^{-/-}$ × *IFNRI*$^{-/-}$ mice exhibited signs of extranuclear localization of HMGB-1, with abundant expression of cytosolic as well as extracellular HMGB-1 (Figure 3B). This was accompanied by infiltration of inflammatory cells and subsequent destruction of cartilage and bone. A clear correlation with clinical scoring was evident (results not shown), in that synovitis in mice with maximal clinical arthritis scores was correlated with the expression of extensive amounts of extracellular HMGB-1. The aberrant overexpression of intraarticular HMGB-1 was also prominent at later time points, when the systemic HMGB-1 levels were strongly reduced or even undetectable.

Cytoplasmic HMGB-1 expression in abnormal macrophages with undigested DNA. Numerous peritoneal macrophages obtained from both healthy and arthritic *DNase II*$^{-/-}$ × *IFNRI*$^{-/-}$ mice contained undigested DNA in multiple, enlarged cytoplasmic vacuoles (Figures 4A and B). Nuclear, as well as diffuse, cytoplasmic HMGB-1 staining was demonstrated in these cells. Most of the lysosomes containing undigested DNA

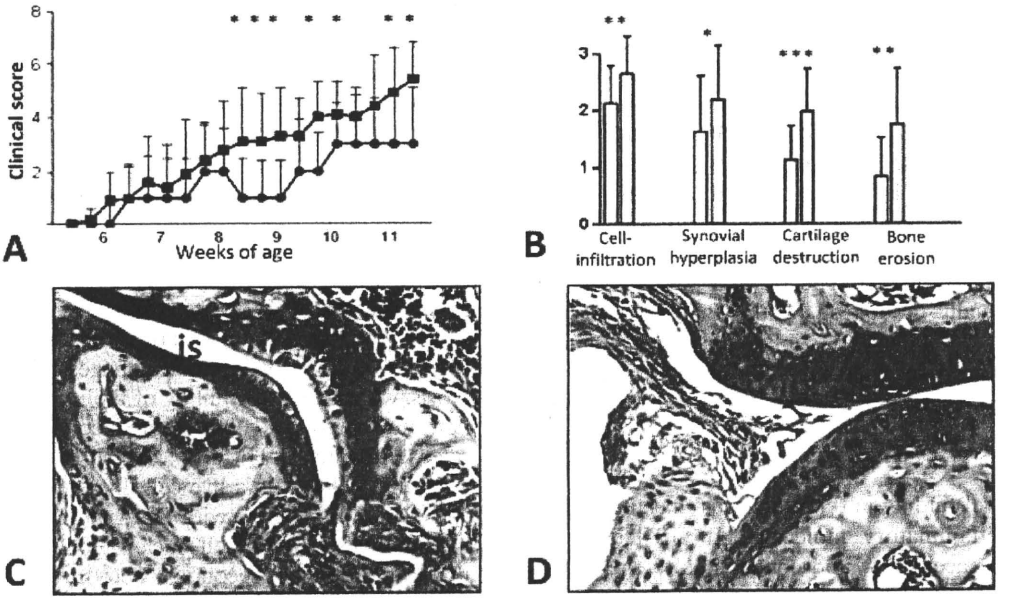

Figure 6. Blocking of high mobility group box chromosomal protein 1 (HMGB-1) expression attenuates clinical arthritis and protects against joint destruction in the murine model. **A,** Disease development was significantly ameliorated in *DNase II*$^{-/-}$ × *IFNRI*$^{-/-}$ mice treated with the HMGB-1–specific antagonist BoxA (n = 7; circles), as compared with control mice treated with vehicle alone (n = 8; squares). **B,** Evaluation of the histopathologic features of the joint specimens for signs of cell infiltration, synovial hyperplasia, cartilage destruction, and bone erosions using a clinical score (on a scale from 0 [normal appearance] to 3 [maximal pathology]) revealed a significantly lower score for all parameters in BoxA-treated mice (open bars) as compared with control mice (shaded bars). Bars in **A** and **B** show the mean and SD. * = $P = 0.05$; ** = $P = 0.01$; *** = $P = 0.005$, between groups. **C** and **D,** Representative photomicrographs illustrate murine articular joints stained with Safranin O after treatment with vehicle (**C**) and after HMGB-1 blocking therapy (**D**). Note the destained cartilage layers in the vehicle-treated joint, reflecting loss of matrix proteoglycans, massive cell infiltration, and synovial hyperplasia invading into subchondral bone (**C**), as compared with the joint of a BoxA-treated mouse in which more homogeneous cartilage staining and preserved joint morphologic features are evident (**D**). **s** = synovial tissue; **js** = joint space; **c** = cartilage (original magnification × 125).

were devoid of detectable HMGB-1 expression. However, HMGB-1 could be demonstrated to be colocalized with DNA in a small fraction of the lysosomal vacuoles (Figures 4A and B).

A majority of the obtained peritoneal macrophages expressed intracellular IL-1β as a sign of activation (Figure 4C). Peritoneal macrophages from wild-type mice exhibited mainly a nuclear HMGB-1 staining pattern and only occasional cells with intracellular IL-1β that was weakly expressed. Spleen tissue sections were also studied, due to the presence of splenomegaly. Numerous abnormal macrophages containing large lysosomal vacuoles with undigested DNA that appeared devoid of HMGB-1 expression were observed in the spleen (Figure 4D).

Development of HMGB-1 autoantibodies in *DNase II* × *IFNRI*–deficient mice. Since anti–HMGB-1 antibodies have been reported in systemic rheumatic diseases (33–35) and may possibly influence the extracellular levels of HMGB-1, we also studied the presence of such antibodies in the animals. HMGB-1 autoantibodies appeared in *DNase II*–deficient mice at the earliest time point studied (6–7 weeks of age), before the onset of arthritis (Figure 5A). Levels of HMGB-1 autoantibodies were maintained at onset of arthritis at 8–9 weeks of age (Figure 5B), and increased at the time of established arthritis at 11–13 weeks of age (Figure 5C). There was a statistically significant correlation between high serum HMGB-1 levels before arthritis and high levels of HMGB-1 autoantibodies after established arthritis ($r^2 = 0.669$, $P = 0.0132$).

Amelioration of arthritis and joint destruction by targeting of HMGB-1. Therapeutic intervention with truncated HMGB-1 BoxA protein has previously yielded beneficial results in collagen-induced arthritis (CIA) in mice and rats (14). Structure-function analysis has dem-

onstrated that the DNA-binding BoxB domain mediates the proinflammatory effects of HMGB-1, while the DNA-binding BoxA has antiinflammatory properties, acting as a competitive antagonist to full-length HMGB-1.

Systemic administration of BoxA protein to *DNase II*$^{-/-}$ × *IFNRI*$^{-/-}$ animals every second day for 5 weeks significantly improved clinical arthritis scores (Figure 6A), and also ameliorated the histologic severity of arthritis and reduced the tissue destruction in these animals (Figures 6B–D). The studied parameters that were beneficially influenced by the BoxA therapy included synovial hyperplasia, inflammatory cell influx, depletion of cartilage matrix, and bone erosions.

DISCUSSION

A novel finding in this study was that the endogenous proinflammatory molecule HMGB-1 is overexpressed extracellularly and contributes to the pathogenesis of polyarthritis in *DNase II*$^{-/-}$ × *IFNRI*$^{-/-}$ mice. The most important finding of the present study is the confirmation of HMGB-1 as a promising target molecule to treat synovitis. Previous experimental studies based on the use of HMGB-1–specific antagonists have all been performed exclusively in models of CIA (14,23). The causes of the development of arthritis in *DNase II* × *IFNRI*–deficient animals are obviously different from those in mice with CIA, and yet antagonistic treatment targeting HMGB-1 or TNF works well in both arthritis models (2,14,36). Neutralizing HMGB-1 in CIA confers significant protection against cartilage and bone destruction, and similar beneficial effects were observed in the present study. This is consistent with previous observations of the inhibition of the expected stimulatory effects of HMGB-1 on osteoclast activation and the proteolytic degradation system (28,30,37). Recombinant BoxA treatment has also been demonstrated to effectively attenuate inflammation and damage in other experimental models of a wide range of inflammatory diseases in which HMGB-1 is implicated in the pathogenesis (14,17,19,38,39).

A central question arising as a result of our findings is the origin of the extracellular HMGB-1 detected in prearthritic and arthritic *DNase II*$^{-/-}$ × *IFNRI*$^{-/-}$ mice. Several mechanisms might be involved, all of which are consistent with our findings. The defect in DNase II enzyme activity in macrophages causes accumulation of undigested DNA in the lysosomes, which somehow activates the cells to produce cytokines. It has previously been demonstrated in these animals that the activated macrophages will produce TNF and IFNβ in a Toll-like receptor (TLR)–independent pathway (40). Our present study extends these findings, as demonstrated by immunostaining of peritoneal macrophages, which showed that activated macrophages also coproduce IL-1β and HMGB-1. Once synovitis is established, it is also obvious, from our studies of synovial tissue sections, that activated macrophages translocate their nuclear HMGB-1 to the cytosol and also extracellularly, which is an expected event in an activated macrophage.

Another source of extracellular HMGB-1 might be found in overloaded macrophages that undergo necrosis, which leads to spilling of their nuclear HMGB-1. Any nucleated cell undergoing necrosis will passively release its nuclear HMGB-1, which is only very weakly adherent to DNA in a live cell. In contrast, HMGB-1 is more stably associated with DNA in an apoptotic cell or in expelled erythroid cell nuclei. However, if apoptotic material undergoes secondary necrosis, it will release its HMGB-1 either as uncomplexed molecules or as those complexed to DNA, nucleosomes, or histones. The abnormal handling of apoptotic DNA in *DNase II*–deficient animals creates a scenario in which these events may take place. In immunostaining studies, we observed that most of the undigested DNA in the lysosomes lacked HMGB-1, probably due to a normal proteolytic system, but extracellular apoptotic bodies not engulfed by the overwhelmed reticuloendothelial system may provide a rich source of HMGB-1. Substantial levels of circulating DNA have been reported in this model (2).

Finally, it was recently demonstrated that hypoxic areas in synovitis will also efficiently release HMGB-1. Indeed, release of HMGB-1 is observed not only in necrotic cells, but also in metabolically stressed cells exposed to even moderate hypoxia (23).

The timing of the systemic and intraarticular aberrant overexpression of HMGB-1 differed distinctly and demonstrated an inverse relationship. The highest HMGB-1 serum levels were recorded prior to and at the onset of clinical disease. The systemic HMGB-1 load then unexpectedly declined, despite the continuous progression of the articular disease, with extensive local HMGB-1 secretion. A similar kinetic pattern regarding serum levels of DNA and TNF has been previously reported (2). We suggest that these results reflect the fact that TNF and HMGB-1, and possibly other proinflammatory cytokines, that are produced by bone marrow macrophages are involved in the initiation of the polyarthritis. Once the synovitis is established, local

intraarticular production of the same mediators, including HMGB-1, is enough to sustain and propagate the polyarthritis. The reason that the joints exclusively are affected by inflammation as a consequence of the systemic triggering is an as yet unresolved question, but it is well known that joint tissue is particularly prone to retain immune complexes, crystals, and other debris not eliminated by a functional reticuloendothelial system (41). The activated and overloaded macrophages of the *DNase II*–deficient mice will undoubtedly provide both proinflammatory cytokines and undigested components that play a role in the initiation of intraarticular inflammation.

One reason for the decline in the systemic pool of extracellular HMGB-1 might be the fact that generation of HMGB-1 autoantibodies takes place, as described herein. The reciprocal relationship between serum levels of HMGB-1 and levels of anti–HMGB-1 antibodies may possibly favor this interpretation. HMGB-1 autoantibodies are commonly detected in systemic rheumatic diseases, but their functional role is unclear (33–35). In one study, the presence of anti–HMGB-1 antibodies correlated with disease activity in patients with systemic lupus erythematosus (42). Whether the autoantibodies generated in the present mouse model are protective by acting to neutralize systemic HMGB-1, or even pathogenetic by forming immune complexes, remains unclear and warrants further studies.

It is important to understand the mechanisms by which extracellular HMGB-1 contributes to articular inflammation. HMGB-1 mediates its inflammatory responses to sterile and infectious threats by signaling via highly conserved receptors, including TLR-2, TLR-4, TLR-9, and the receptor for advanced glycation end products (43–45). Furthermore, HMGB-1 has an inherent ability to form complexes with other molecules, such as IL-1β, nucleosomes, and bacterial DNA (44,46,47). These complexes then generate inflammation in a synergistic manner. Nucleosomes complexed to HMGB-1 are powerful proinflammatory mediators, whereas uncoupled nucleosomes are immunologically inert (48). In addition, it has recently been described that cytoplasmic HMGB proteins function as universal sentinels for nucleic acid–mediated innate immune responses and are essential for type I IFN production (49). The as yet unexplained excessive production of IFNβ in *DNase II*–deficient mice might thus be attributed to intracellular HMGB-1–DNA interactions in the macrophages.

The HMGB-1 BoxA domain is identical in all mammals. Therapy based on this truncated protein has now been proven beneficial in 2 separate models of polyarthritis and in a number of other inflammatory conditions in which HMGB-1 is involved. These encouraging results have been obtained despite the fact that the recombinant protein has a very short lifespan in the circulation. It is plausible that the therapeutic potential of this molecule could be even greater after modifications are made to prolong its biologic availability. Taken together, these results indicate that the strategy to counteract HMGB-1 provides an interesting opportunity for future clinical trials in the treatment of chronic arthritis.

AUTHOR CONTRIBUTIONS

All authors were involved in drafting the article or revising it critically for important intellectual content, and all authors approved the final version to be published. Dr. Palmblad had full access to all of the data in the study and takes responsibility for the integrity of the data and the accuracy of the data analysis.

Study conception and design. Östberg, Klevenvall, Bianchi, Harris, Andersson, Palmblad.

Acquisition of data. Östberg, Yang, Klevenvall, Palmblad.

Analysis and interpretation of data. Östberg, Kawane, Nagata,Yang, Chavan, Klevenvall, Bianchi, Harris, Andersson, Palmblad.

REFERENCES

1. Van den Berg WB. Lessons from animal models of arthritis over the past decade. Arthritis Res Ther 2009;11:250–60.
2. Kawane K, Ohtani M, Miwa K, Kizawa T, Kanbara Y, Yoshioka Y, et al. Chronic polyarthritis caused by mammalian DNA that escapes from degradation in macrophages. Nature 2006;443:998–1002.
3. Evans CJ, Aguilera RJ. DNase II: genes, enzymes and function. Gene 2003;322:1–15.
4. Kawane K, Fukuyama H, Yoshida H, Nagase H, Ohsawa Y, Uchiyama Y, et al. Impaired thymic development in mouse embryos deficient in apoptotic DNA degradation. Nat Immunol 2003;4:138–44.
5. Yoshida H, Okabe Y, Kawane K, Fukuyama H, Nagata S. Lethal anemia caused by interferon-β produced in mouse embryos carrying undigested DNA. Nat Immunol 2005;6:49–56.
6. Bustin M, Reeves R. High-mobility-group chromosomal proteins: architectural components that facilitate chromatin function. Prog Nucleic Acid Res Mol Biol 1996;54:35–100.
7. Park JS, Arcaroli J, Yum HK, Yang H, Wang H, Yang KY, et al. Activation of gene expression in human neutrophils by high mobility group box 1 protein. Am J Physiol Cell Physiol 2003;284:C870–9.
8. Gardella S, Andrei C, Ferrera D, Lotti LV, Torrisi MR, Bianchi ME, et al. The nuclear protein HMGB1 is secreted by monocytes via a non-classical, vesicle-mediated secretory pathway. EMBO Rep 2002;13:995–1001.
9. Bonaldi T, Talamo F, Scaffidi P, Ferrera D, Porto A, Bachi A, et al. Monocytic cells hyperacetylate chromatin protein HMGB1 to redirect it towards secretion. EMBO J 2003;22:5551–60.
10. Dumitriu IE, Baruah P, Valentinis B, Voll RE, Herrmann M, Nawroth PP, et al. Release of high mobility group box 1 by dendritic cells controls T cell activation via the receptor for advanced glycation end products. J Immunol 2005;174:7506–15.
11. Semino C, Angelini G, Poggi A, Rubartelli A. NK/iDC interaction results in IL-18 secretion by DCs at the synaptic cleft followed by NK cell activation and release of the DC maturation factor HMGB1. Blood 2005;106:609–16.
12. Scaffidi P, Misteli T, Bianchi ME. Release of chromatin protein

HMGB1 by necrotic cells triggers inflammation. Nature 2002;418:191–5.
13. Bell CW, Jiang W, Reich CF III, Pisetsky DS. The extracellular release of HMGB1 during apoptotic cell death. Am J Physiol Cell Physiol 2006;291:C1318–25.
14. Kokkola R, Li J, Sundberg E, Aveberger AC, Palmblad K, Yang H, et al. Successful treatment of collagen-induced arthritis in mice and rats by targeting extracellular high mobility group box chromosomal protein 1 activity. Arthritis Rheum 2003;48:2052–8.
15. Maeda S, Hikiba Y, Shibata W, Ohmae T, Yanai A, Ogura K, et al. Essential roles of high-mobility group box 1 in the development of murine colitis and colitis-associated cancer. Biochem Biophys Res Commun 2007;360:394–400.
16. Tsung A, Sahai R, Tanaka H, Nakao A, Fink MP, Lotze MT, et al. The nuclear factor HMGB1 mediates hepatic injury after murine liver ischemia-reperfusion. J Exp Med 2005;201:1135–43.
17. Andrassy M, Volz HC, Igwe JC, Funke B, Eichberger SN, Kaya Z, et al. High-mobility group box-1 in ischemia-reperfusion injury of the heart. Circulation 2008;117:3216–26.
18. Ellerman JE, Brown CK, de Vera M, Zeh HJ, Billiar T, Rubartelli A, et al. Masquerader: high mobility group box-1 and cancer. Clin Cancer Res 2007;13:2836–48.
19. Yang H, Ochani M, Li J, Qiang X, Tanovic M, Harris HE, et al. Reversing established sepsis with antagonists of endogenous high-mobility group box 1. Proc Natl Acad Sci U S A 2004;101:296–301.
20. Jiang W, Pisetsky DS. Mechanisms of disease: the role of high-mobility group protein 1 in the pathogenesis of inflammatory arthritis. Nat Clin Pract Rheumatol 2007;3:52–8.
21. Taniguchi N, Kawahara K, Yone K, Hashiguchi T, Yamakuchi M, Goto M, et al. High mobility group box chromosomal protein 1 plays a role in the pathogenesis of rheumatoid arthritis as a novel cytokine. Arthritis Rheum 2003;48:971–81.
22. Palmblad K, Sundberg E, Diez M, Soderling R, Aveberger AC, Andersson U, et al. Morphological characterization of intra-articular HMGB1 expression during the course of collagen-induced arthritis. Arthritis Res Ther 2007;9:R35.
23. Hamada T, Torikai M, Kuwazuru A, Tanaka M, Horai N, Fukuda T, et al. Extracellular high mobility group box chromosomal protein 1 is a coupling factor for hypoxia and inflammation in arthritis. Arthritis Rheum 2008;58:2675–85.
24. Pullerits R, Jonsson IM, Verdrengh M, Bokarewa M, Andersson U, Erlandsson-Harris H, et al. High mobility group chromosomal protein 1, a DNA binding cytokine, induces arthritis. Arthritis Rheum 2003;48:1693–700.
25. Andersson U, Wang H, Palmblad K, Aveberger AC, Bloom O, Erlandsson-Harris H, et al. HMG-1 stimulates proinflammatory cytokine synthesis in human monocytes. J Exp Med 2000;192:565–70.
26. Parkkinen J, Raulo E, Merenmies J, Nolo R, Kajander EO, Baumann M, et al. Amphoterin, the 30-kDa family of HMG1-type polypeptides: enhanced expression in transformed cells, leading edge localization, and interactions with plasminogen activation. J Biol Chem 1993;268:19726–38.
27. Taguchi A, Blood DC, del Toro G, Canet A, Lee DC, Qu W, et al. Blockade of RAGE-amphoterin signalling suppresses tumour growth and metastases. Nature 2000;405:354–9.
28. Zhou Z, Han JY, Xi CX, Xie JX, Feng X, Wang CY, et al. HMGB1 regulates RANKL-induced osteoclastogenesis in a manner dependent on RAGE. J Bone Miner Res 2008;23:1084–96.
29. Yamoah K, Brebene A, Baliram R, Inagaki K, Dolios G, Arabi A, et al. High-mobility group box proteins modulate tumor necrosis factor-α expression in osteoclastogenesis via a novel deoxyribonucleic acid sequence. Mol Endocrinol 2008;22:1141–53.
30. Yang J, Shah R, Robling AG, Templeton E, Yang H, Tracey KJ, et al. HMGB1 is a bone-active cytokine. J Cell Physiol 2008;214:730–9.
31. Joosten LA, Helsen MM, Saxne T, van de Loo FA, Heinegard D, van den Berg WB. IL-1$\alpha\beta$ blockade prevents cartilage and bone destruction in murine type II collagen-induced arthritis, whereas TNF-α blockade only ameliorates joint inflammation. J Immunol 1999;163:5049–55.
32. Wang H, Bloom O, Zhang M, Vishnubhakat JM, Ombrellino M, Che J, et al. HMG-1 as a late mediator of endotoxin lethality in mice. Science 1999;285:248–51.
33. Wittemann B, Neuer G, Michels H, Truckenbrodt H, Bautz FA. Autoantibodies to nonhistone chromosomal proteins HMG-1 and HMG-2 in sera of patients with juvenile rheumatoid arthritis. Arthritis Rheum 1990;33:1378–83.
34. Burlingame RW, Rubin RL, Rosenberg AM. Autoantibodies to chromatin components in juvenile rheumatoid arthritis. Arthritis Rheum 1993;36:836–41.
35. Uesugi H, Ozaki S, Sobajima J, Osakada F, Shirakawa H, Yoshida M, et al. Prevalence and characterization of novel pANCA, antibodies to the high mobility group non-histone chromosomal proteins HMG1 and HMG2, in systemic rheumatic diseases. J Rheumatol 1998;25:703–9.
36. Williams RO, Feldmann M, Maini RN. Anti-tumor necrosis factor ameliorates joint disease in murine collagen-induced arthritis. Proc Natl Acad Sci U S A 1992;89:9784–8.
37. Taniguchi N, Yoshida K, Ito T, Tsuda M, Mishima Y, Furumatsu T, et al. Stage-specific secretion of HMGB1 in cartilage regulates endochondral ossification. Mol Cell Biol 2007;27:5650–63.
38. Gong Q, Xu JF, Yin H, Liu SF, Duan LH, Bian ZL. Protective effect of antagonist of high-mobility group box 1 on lipopolysaccharide-induced acute lung injury in mice. Scand J Immunol 2009;69:29–35.
39. Muhammad S, Barakat W, Stoyanov S, Murikinati S, Yang H, Tracey KJ, et al. The HMGB1 receptor RAGE mediates ischemic brain damage. J Neurosci 2008;28:12023–31.
40. Okabe Y, Kawane K, Akira S, Taniguchi T, Nagata S. Toll-like receptor-independent gene induction program activated by mammalian DNA escaped from apoptotic DNA degradation. J Exp Med 2005;202:1333–9.
41. Schulz LC, Schaening U, Pena M, Hermanns W. Borderline-tissues as sites of antigen deposition and persistence—a unifying concept of rheumatoid inflammation? Rheumatol Int 1985;5:221–7.
42. Hayashi A, Nagafuchi H, Ito I, Hirota K, Yoshida M, Ozaki S. Lupus antibodies to the HMGB1 chromosomal protein: epitope mapping and association with disease activity. Mod Rheumatol 2009;19:283–92.
43. Yu M, Wang H, Ding A, Golenbock DT, Latz E, Czura CJ, et al. HMGB1 signals through Toll-like receptor (TLR) 4 and TLR2. Shock 2006;26:174–9.
44. Tian J, Avalos AM, Mao SY, Chen B, Senthil K, Wu H, et al. Toll-like receptor 9-dependent activation by DNA-containing immune complexes is mediated by HMGB1 and RAGE. Nat Immunol 2007;8:487–96.
45. Hori O, Brett J, Slattery T, Cao R, Zhang J, Chen JX, et al. The receptor for advanced glycation end products (RAGE) is a cellular binding site for amphoterin: mediation of neurite outgrowth and co-expression of RAGE and amphoterin in the developing nervous system. J Biol Chem 1995;270:25752–61.
46. Sha Y, Zmijewski J, Xu Z, Abraham E. HMGB1 develops enhanced proinflammatory activity by binding to cytokines. J Immunol 2008;180:2531–7.
47. Hreggvidsdottir HS, Ostberg T, Wahamaa H, Schierbeck H, Aveberger AC, Klevenvall L, et al. The alarmin HMGB1 acts in synergy with endogenous and exogenous danger signals to promote inflammation. J Leukoc Biol 2009;88:655–62.
48. Urbonaviciute V, Furnrohr BG, Meister S, Munoz L, Heyder P, De Marchis F, et al. Induction of inflammatory and immune responses by HMGB1-nucleosome complexes: implications for the pathogenesis of SLE. J Exp Med 2008;205:3007–18.
49. Yanai H, Ban T, Wang Z, Choi MK, Kawamura T, Negishi H, et al. HMGB proteins function as universal sentinels for nucleic-acid-mediated innate immune responses. Nature 2009;462:99–103.

Ann. N.Y. Acad. Sci. ISSN 0077-8923

ANNALS OF THE NEW YORK ACADEMY OF SCIENCES
Issue: *Clearance of Dying Cells in Healthy and Diseased Immune Systems*

Apoptosis and autoimmune diseases

Shigekazu Nagata[1,2]

[1]Department of Medical Chemistry, Graduate School of Medicine, University of Kyoto, Yoshida, Konoe, Sakyo, Kyoto, Japan. [2]Core Research for Evolutional Science and Technology, Japanese Science and Technology Agency, Kyoto, Yoshida, Konoe, Sakyo, Kyoto, Japan

Address for correspondence: Shigekazu Nagata, Ph.D., Department of Medical Chemistry, Graduate School of Medicine, University of Kyoto, Yoshida-Konoe, Sakyo-ku, Kyoto 606-8501, Japan. snagata@mfour.med.kyoto-u.ac.jp

Every day billions of cells die in our bodies to eliminate those that are harmful, useless, or senescent. The process can be divided into two steps: cell dying and cell clearance. In the first step, death machinery is activated in the cells and quickly kills them. During the second step, dead cells are engulfed by phagocytes, and their components are degraded in the lysosomes of the phagocytes. The death mechanism and the clearance of dead cells have been extensively studied. Mouse lines that are deficient in the death or clearance process have been established, and human patients carrying a mutation in the death machinery have been identified. Data from these mutant mice and human patients indicate that defects in cell death or dead-cell clearance leads to autoimmunity. This review examines the cell death and clearance processes and briefly discusses the diseases they cause.

Keywords: apoptosis; caspase; DNA degradation; macrophages; autoimmune disease; erythropoiesis

Cell death

During the development of metazoans, many useless and/or toxic cells are generated and removed.[1–3] In the adult, senescent cells die and are replaced by newly generated ones. In effect, different cell types have different life spans: less than 2 days for neutrophils in the bloodstream, 150 days for hepatocytes, and years to decades for heart-muscle cells and neurons. Because our bodies carry 1.5×10^{10} neutrophils in the bloodstream, about 10^{10} neutrophils die each day.

Among the several cell-death processes, apoptosis has the distinction of being a "clean" process—that is, during apoptotic cell death, none of their components are released into the extracellular space.[4] Thus, in this process, the membranes of the dying cells convolute and nuclei become condensed and fragmented. In the final stage of this process, the cells themselves become fragmented, but the fragments are enclosed by the plasma membranes, which remain intact. The condensed and fragmented cells are then engulfed by phagocytes, transferred to the lysosomes, and degraded by lysosomal proteases, nucleases, and glycosidases into amino acids, nucleotides, and sugar moieties.[5] In contrast, during necrosis, the nuclei and mitochondria swell, rupturing the cell membrane and releasing the contents of the dead cells into the extracellular space.

Cells use energy to maintain the integrity of their plasma membranes. For example, various ATP-dependent enzymes work to maintain the asymmetrical distribution of phospholipids across the inner and outer leaflets of the lipid bilayer. In the necrotic process, ATP is quickly released from the dying cells, whereas a high ATP level is thought to be maintained in apoptotic cells.[6] However, because the function of the mitochondria is destroyed in apoptosis, the apoptotic cells also lose ATP. This will cause the disintegration and rupture of the plasma membrane,[7] leading to secondary necrosis.

Most of the physiological cell death that occurs in mammalian development seems to proceed via apoptosis, for which two pathways have been elucidated: the intrinsic and extrinsic pathways.[1] In the intrinsic death pathway, at least one BH3-only protein such as Bim, is activated in the cells, and

doi: 10.1111/j.1749-6632.2010.05749.x

Ann. N.Y. Acad. Sci. 1209 (2010) 10–16